BRIMROSE Technology Corporation
P.O. Box 616, 19 Loveton Circle, Sparks, Maryland 21152-9201
Phone: 410-472-2600; Fax: 410-472-7960; www.brimrosetechnology.com

Next Generation Semiconductor-Based Radiation Detectors Using Cadmium Magnesium Telluride

Phase I Grant - DE-SC0011328
(Purchase Request or Funding Document No.: 14SC500368)

EXECUTIVE SUMMARY

The Office of Defense Nuclear Nonproliferation Research and Development is focused on enabling the development of next generation gamma radiation detectors that are rugged, reliable, low power and capable of high-confidence radioisotope identification. The primary objective of the Phase I program was to perform extensive studies on the purification, crystal growth and post-growth annealing/processing procedures of Cadmium Magnesium Telluride (CdMgTe) to gain a clear understanding of the basic material properties to produce detector material with better or comparable performance at lower cost than that of Cadmium Zinc Telluride (the current material of choice for gamma ray detection). Key issues which play important role in this materials development effort are combination of high resistivity and high mobility-life time product. These parameters in turn depend upon the band-gap, purity and defects in the material. In optimizing detector materials, a good control of high purity and defects will allow control of mobility-life time product and control of sensitivity and resolution of the detector

During this STTR program, processing techniques for these crystals including purification, crystal growth, annealing, mechanical and chemical polishing, surface passivation and electrode fabrication were investigated. Techniques to characterize pertinent electronic characteristics were developed in-house and gamma ray detectors were fabricated and tested using suitable crystals to validate our characterization techniques. Feasibility of the development of comprehensive defect modeling in this new class of material was demonstrated by our partner research institute SRI, to compliment the experimental work.

We successfully produced CdMgTe material with resistivity of 3.12×10^{10} Ohm-cm and $\mu\tau = 5.3 \times 10^{-3}$ cm^2/V. Our material showed 662 keV gamma responses from a 4 x 4 x 10 mm^3 Pseudo Frisch-Grid CdMgTe detector with energy resolution of 3.4% (FWHM) at room temperature, without any additional signal correction. These results are comparable to existing CdZnTe (CZT) technology using the same detector size and testing conditions. Thus in Phase I we have successfully demonstrated detection of gamma-radiation from various isotopes/sources, using CdMgTe that was comparable to that of CdZnTe, thus clearly proving the feasibility that CdMgTe is an excellent, low-cost alternative to CdZnTe.

DOE/11172015-Final

Next Generation Semiconductor-Based Radiation Detectors Using Cadmium Magnesium Telluride

Final Report

February 18, 2014 – November 17, 2014

Brimrose Technology Corporation
19 Loveton Circle
Sparks, Maryland 21152-9201

Key Personnel
Brimrose Technology Corporation

Dr. Sudhir B. Trivedi
Dr. Susan W. Kutcher
Dr. Witold Palsoz

Dr. Martha Berding
SRI International
Subcontractor

Dr. Arnold Burger
Consultant

November 17, 2014

Prepared for

THE U.S. DEPARTMENT OF ENERGY
Under Grant Award – DE-SC0011328

Report contains "No proprietary information"

Next Generation Semiconductor-Based Radiation Detectors Using Cadmium Magnesium Telluride

Phase I Grant - DE-SC0011328
(Purchase Request or Funding Document No.: 14SC500368)

ACKNOWLEDGEMENTS

We acknowledge and extend our sincerest appreciation to the Department Of Energy Program Technical Monitor, Dr. David Beach for his constant interest and support in development of the novel CdMgTe material as a possible alternative to CdZnTe material for Room Temperature Gamma Ray Detection.

The support and efforts of Dr. P.S. Wijewarnasuriya and Mr. James Pattison of, The Army Research Laboratory, Adelphi, Maryland, for their help in the measurement of electronic and optical properties of CdMgTe crystals is acknowledged. Dr. Marc Litz and Dr. Jarod Marsh of, The Army Research Laboratory assisted in the initial radiation measurements on CdMgTe detector crystals, which we gratefully acknowledge.

The dedication of Brimrose Research & Development team members, Mr. David Meyers for an excellent job on mechanical polishing of the CdMgTe detector samples and Mr. Robert Rosemeier and Mr. Cory Rosemeier who assisted with crystal growth, annealing and dicing the crystals, is appreciated.

A special acknowledgement and note of appreciation to the staff members of the contracting division of the Office Of Science and the Department Of Energy SBIR/STTR support desk team, all of which have been extremely helpful throughout this program.

Finally, we gratefully acknowledge the hard work and constant assistance of Ms. Diane Murray, at Brimrose during the entire program. Our sincere thanks to her for the efficient administration of the contract and incessant help in preparation of the final report and Phase II proposal

Next Generation Semiconductor-Based Radiation Detectors Using Cadmium Magnesium Telluride

Phase I Grant - DE-SC0011328
(Purchase Request or Funding Document No.: 14SC500368)

TABLE OF CONTENTS

LIST OF FIGURES

LIST OF TABLES

Table **Page**

Next Generation Semiconductor-Based Radiation Detectors Using Cadmium Magnesium Telluride

Phase I Grant - DE-SC0011328
(Purchase Request or Funding Document No.: 14SC500368)

FINAL REPORT

1.0 Introduction

Semiconductor radiation detectors, operating at room temperature, have remained the subject of great interest and importance for DOE and DOD to enforce proliferation and also counter possible radiological and nuclear threats from terrorists. Cryogenically operating, high-purity germanium (HPGe) is the dominant semiconductor radiation detector material and is considered a gold standard. HPGe semiconductor detectors have the highest resolution and are the only solution available for many high-performance applications. However, their cost is prohibitively high for majority of security applications. The combination of cryogenic operation and prohibitive cost severely limits the use of these detectors to mostly stationary or laboratory based applications and unsuitable for large scale US port protection. Therefore, there is a desperate need for low-cost, direct detection room-temperature semiconductor detector (RTSD) material for mobile, high-resolution applications.

Cadmium zinc telluride (CdZnTe or CZT) is currently the accepted material of choice, and reasonable alternative to HPGe for most applications, for room temperature radiation detection. However, CZT , due to wide separation between solidus and liquidus, in its pseudo binary phase diagram, results in poor crystal growth yields which in turn results into the cost that is several times higher than that of HPGe (already much more expensive than the scintillators). As a result, CZT is considered much too expensive, except in those applications where the form factor of the detector is critical, such as mobile domestic security and military applications. For practical applications, production of CZT crystals in large sizes (> 2inches in diameter) with high yield and low production cost is essential to realize critical applications which need high volume/high resolution detector crystals. Consequently, for years the US government as well as the scientific community has been calling for alternative, cost effective, material that can potentially provide comparable or better performance than CdZnTe.

The Office of Defense Nuclear Nonproliferation Research and Development is focused on enabling the development of next generation gamma radiation detectors that are rugged, reliable, low power and capable of high-confidence radioisotope identification. Currently, the program is focused on the development of improved capabilities for radiation detectors, with the objective being to gain insight into the mechanistic understanding of material performance. To enhance the understanding of these mechanisms requires a **better understanding of basic materials properties and techniques to produce and process them.**

The material that is the subject of this work is the II-VI semiconductor cadmium magnesium telluride (CdMgTe). The primary objective of the Phase I program was to perform extensive

studies on the purification, crystal growth and post-growth annealing/processing procedures of (CdMgTe) to gain a clear understanding of the basic material properties to produce detector material with better or comparable performance than that of CZT. Key issues which play important role in this materials development effort are combination of high resistivity and high mobility-life time product. These parameters in turn depend upon the band-gap, purity and defects in the material. In optimizing detector materials, a good control of high purity and defects will allow control of mobility-life time product and control of sensitivity and resolution of the detector

Additionally, compound semiconductors with bandgap in the range of 1.35 – 2.55 eV are generally of interest for radiation detector applications since the wide bandgap will allow room temperature operation and reduced dark leakage current. CdMgTe's bandgap is tunable and is wider than that of CZT. Wider bandgap leads to lower dark leakage current, a very important advantage that CdMgTe has over CZT in term of compatibility with currently available electronics, specifically, ASIC electronics or Applications Specific Integrated Circuits. Having a level of dark leakage current that is higher than what the ASIC can handle has been a major factor limiting the wide deployment of CZT detectors in applications where detector arrays (as with pixelated devices) are needed.

During this STTR program, Brimrose utilized their prior experience and expertise in the growth and processing of II-VI crystals and produced high purity material and good quality single crystals of CdMgTe. Processing techniques for these crystals including, annealing, mechanical and chemical polishing, surface passivation and electrode fabrication were developed. Techniques to characterize pertinent electronic characteristics were developed in-house and gamma ray detectors were fabricated and tested using suitable crystals to validate our characterization techniques. Feasibility of the development of comprehensive defect modeling in this new class of material was demonstrated by our partner research institute SRI, to compliment the experimental work. In light of the time constraint and limited knowledge of pressure-temperature phase diagram in CdMgTe material, the bread board of modeling was developed which will be further optimized during Phase II.

Our ultimate goal in this program was the low cost production of CdMgTe crystals with resistivity $\geq 10^{11}$ ohm-cm and to demonstrate $\mu\tau > 10^{-3}$ cm^2/V, achieving 10^{-2} cm^2/V. During this Phase I STTR program we have produced CdMgTe material with **resistivity of 3.12 x 10^{10} Ohm-cm** and **$\mu\tau$ = 5.3 x 10^{-3} cm^2/V**. Our material showed 662 keV gamma responses from a 4 x 4 x 10 mm^3 Pseudo Frisch-Grid CdMgTe detector with energy resolution of 3.4% (FWHM) at room temperature, without any additional signal correction. ***These results are comparable to existing CdZnTe (CZT) technology using the same detector size and testing conditions. Thus in Phase I we have successfully demonstrated detection of gamma-radiation from various isotopes/sources, using CdMgTe that was comparable to that of CdZnTe, thus clearly proving the feasibility that CdMgTe is an excellent, low-cost alternative to CdZnTe.***

Through understanding we gained through current purification, growth and doping studies, coupled with defect modeling studies we will further optimize the materials parameters and processing techniques necessary to produce material suitable for high efficiency, high resolution gamma-ray detection during Phase II program.

2.0 Background and Rational

Material Properties of Importance

The material property that is of most consequence to the successful operation of radiation detection material is the electron-hole transport properties: **Good transport properties translate to a large mobility-lifetime product, $\mu\tau$.** The typical target for $\mu\tau$ for electrons in compound semiconductors suitable for gamma ray detection is in the range of 10^{-2} to 10^{-3} $cm^2/(V \cdot s)$**.** Large $\mu\tau$ leads to improved charge collection efficiency. In fact, it has been determined that $\mu\tau$ is the most significant figure of merit for compound semiconductor-based radiation detectors [1]. Mobility is an intrinsic property of the material; therefore, ***lifetime*** becomes the more important parameter. Therefore, in order to improve $\mu\tau$, the lifetime must be optimized, and the lifetime primarily depends on the concentration of defects because they act as charge carrier traps. Therefore, u**nderstanding these defects and their removal/reduction is essential to improving the $\mu\tau$ of the material**.

The formation of defects primarily occurs during material preparation and crystal growth. Therefore, crystal growth must be optimized so as to minimize intrinsic and foreign defect levels as well as extended defects such as dislocations and stacking faults. Although these extended defects can be minimized during crystal growth, native point defects (such as interstitials, vacancies and anti-sites) will always be present in as-grown crystals. The density of each class of defect is determined by the thermodynamic conditions during growth, such as the temperature at the growth front and the chemical potentials of the constituents in the liquid from which the crystal is being grown. These native defects, and their detrimental contribution to the carrier lifetimes, can be manipulated through *post-growth annealing* procedures.

Defect modeling is an excellent way to predict how annealing conditions affect the defect densities. The formation energies of defects can be modeled, and the defect concentrations throughout the existence region of the CdMgTe phase diagram can be calculated. These calculations can then be used to identify annealing conditions that will result in material with long carrier lifetimes. Hence, modeling can be used to determine the optimal a post-growth anneal strategy and control both the temperature and the constituent partial pressures to manipulate the native defect densities and thereby achieve highly intrinsic material.

Other material properties that are important for successful radiation detection are high resistivity and good compositional homogeneity. High resistivity is required to minimize the dark (leakage) current and ensure that the detector can operate at room temperature. In order to produce device quality γ–ray detectors**,** material should have target resistivity $\geq 10^{11}$ ohm-cm. Compositionally homogeneous material is needed to ensure a uniform response throughout the volume of the detector.

Choice of Material: Why CdMgTe?

Currently, cadmium zinc telluride (CZT) is the material of choice for making room temperature γ-ray detectors [2-5]. Detectors based on CZT single crystals are very promising because they combine low noise levels with relatively high charge-carrier properties. The resistivity of $Cd_{0.90}Zn_{0.10}Te$ has been reported to be between 10^8 and 10^{11} Ω-cm [6, 7]. However, the large separation between liquidus and solidus lines in the CdTe-ZnTe phase diagram, makes CZT crystals difficult to grow and it is challenging to yield compositionally homogeneous samples of large size (the segregation coefficient of Zn in CdTe is reported to be approximately 1.3 [8]). Also, problems related to stoichiometry [9] lead to non-uniform response of the devices. Therefore, detectors based on CZT can achieve resolutions of only 2-3 percent and only in rare cases the performance is around or just below 1%.

In 1999, we proposed and demonstrated an alternative wide band gap semiconductor CdMnTe for gamma-ray detection [10]. This material has at least three advantages over CZT: (1) The crystals can have high band gap, which addresses the problem of leakage current; (2) CdTe-MnTe phase diagram solidus and liquidus lines are collinear up to about 30 % of MnTe so the resulting segregation coefficient is close to unity [10]; and (3) the amount of MnTe required in CdTe to have the same energy band gap as CZT is less, thus reducing alloy scattering and improving μτ. In a comparative review article, study of the European Space Agency (ESA) [Owens et al- "Compound semiconductor radiation detectors"], CdMnTe material was mentioned among the few select novel materials to show spectroscopic results at x-ray wavelengths [1].

However, some disadvantages exist for using CdMnTe as gamma ray detection material. The ionicity of bonds in CdMnTe is slightly higher than that in CZT. In general, with II-VI semiconductor compounds, a higher ionicity leads to a higher tendency to crystallization in the hexagonal structure [8]. So, although CdMnTe crystallizes in the zinc-blende structure, it is possible that there could be small hexagonal inclusions. Furthermore, a higher tendency toward twinning compared to CZT has been observed [8]. The occurrence of impurities, defects, and twinning leads to a significant amount of alloy scattering which in turn degrades the charge transport properties.

Recently, $CdTe_{(1-x)}Se_x$ has been considered as an alternative gamma ray detector material [11]. Up to x=0.2 the material crystallizes in zincblende structure and has no separation between solidus and liquidus of CdTe-CdSe pseudo-binary phase diagram, which will ensure segregation free homogeneous material. However, up to x=0.2 the energy band gap reduces and goes below the energy band gap of CdTe resulting in higher surface leakage currents. Moreover selenium is not commercially available in high purity form and is difficult to purify further, thus increasing the cost factor

.

Brimrose had summarized their binary and ternary II-VI bulk semiconductor materials/crystals activities for photonic applications in 2008 [12] where the possibility of CdMgTe room temperature gamma detection and other photonic applications were indicated. In September 2011 Brimrose applied for a DOE SBIR (Grant#10962720) under topic # 35a, titled:
"Development of The Novel Wide Band Gap Semiconductor Materials CdMgTe for Gamma Ray Detection," which was not funded. Around the same time Brimrose received an SBIR Phase I

Program (Contract #FA8650-11-C-5116) from Air Force Research Laboratory at Wright Patterson Air Force Base titled, "Development of CdMgTe and CdMgSe for Optical Switching Applications," which also resulted into a Phase II program. Upon developing good quality CdMgTe crystal growth technology for optical switching, (which required undoped, high purity intrinsic material), we again focused on developing CdMgTe as a room temperature gamma ray detector material. Gamma ray applications need a combination of high resistivity and mobility-life time material, which for producibility requires external doping with a close control on defect centers. This requires suitable doping strategies, and understanding of defect centers and their interactions with surroundings in the host crystal lattice. With our expertise in II-VI materials growth and processing we started collaborating with SRI International (Point Of Contact: Dr. Martha Berding) who has a great deal of expertise and experience in defect modeling and control in II-VI semiconductors We again applied for a DOE Grant, this time under the STTR program. We received the award, which resulted into this program. Meanwhile, Brookhaven National Laboratory published [13] their first report on development of CdMgTe as room temperature X-ray and gamma ray detector material, with modest results. During the current STTR program, Brimrose has advanced CdMgTe gamma ray material beyond BNL results (as reported later in the report) and has demonstrated the feasibility of this material being a viable alternative material to the current "gold standard" material for room temperature gamma ray detection, CdZnTe.

In the present work, where we are proposing an innovative wide band-gap semiconductor, cadmium magnesium telluride (CdMgTe), which has several advantages over CZT:

- The amount of MgTe required in CdTe to have the same energy band gap is less, thus the alloy disorder scattering is lower resulting into better charge transport properties [14];
- Much lower to No segregation [14] of Mg results in improved structural properties and a higher yield of compositionally homogeneous;
- The interatomic distance for Cd-Te and Mg-Te are nearly equal;
- CdMgTe has a band gap that extends into the visible range (Figure 1), and the crystals have interesting physical, optical and non-linear optical properties thereby making them of interest for numerous applications and devices [15-17].

In this Phase I work, we demonstrated that CdMgTe is an excellent candidate as a detector material for next-generation, room temperature gamma-radiation detection systems.

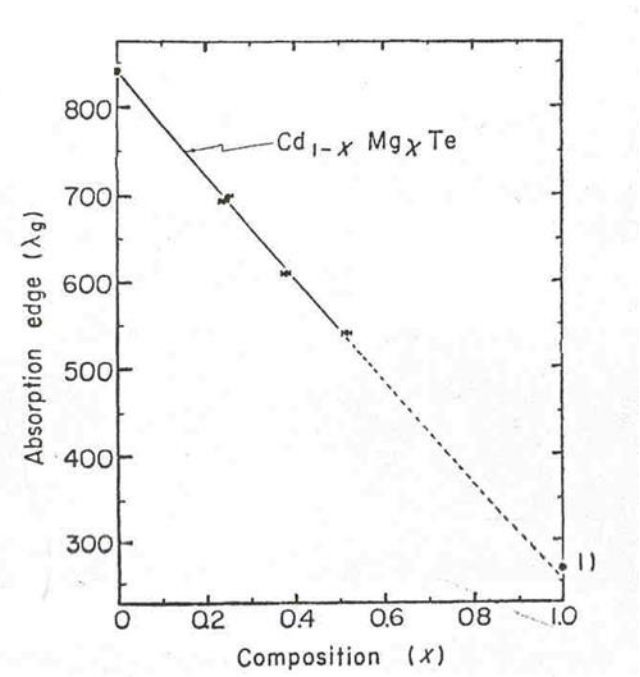

Figure 1. Absorption edge versus composition in $Cd_{(1-x)}Mg_xTe$ [14].

3.0 Summary of Results

In an effort to explore CdMgTe as a potential gamma-ray detector material, we performed extensive studies to gain a clear understanding of the basic material properties and their relation to material performance. The first thing that is necessary in order to achieve device-grade crystal is that starting materials must be extremely pure (better than 6N, 99.9999%). We used a proprietary process that was developed exclusively at Brimrose to purify the starting materials to the highest level possible.

In view of limited time during the Phase I program, we purchased commercially, 7N (99.99999%) pure Cd and Te. We focused instead on purifying the Mg which is available only with purity of 99.98 to 99.99%. During this program using our proprietary technique, described later in the report, we could purify Mg to 99.9999% purity (6N). The chemical assay of our purified material was done by an independent vendor and the analysis report is included later in the report.

The next requirement for production of device quality material is that the grown single crystals must be compositionally homogeneous, free of precipitates or second phases, and contain minimal intrinsic and foreign defect levels. The researchers at Brimrose Technology have over 75 years of combined experience in the area of II-VI crystal growth. This knowledge was used to improve crystal growth for minimal extended defects such as inclusions/precipitates, stacking faults and twins. Numerous crystals were grown via the vertical Bridgman technique with nominal composition of $Cd_{0.92}Mg_{0.08}Te$. Various dopants such as Ge, Er, In, and Fe, were used.

To determine the best post-growth annealing procedures, defect modeling was performed by the researchers at SRI International. SRI has extensive experience on the formation energies of defects in II-VI materials. A thermodynamic code to predict the density of impurities and native

defects in the CdMgTe matrix as a function of equilibration conditions was developed. Un-doped, p-doped, n-doped, and material with deep acceptors or donors in the lattice were explored, the effect on the defect concentrations as the equilibration temperature and cadmium partial pressure were varied was examined.

Brimrose provided SRI with three annealing temperature conditions: 700^0C, 900^0C, and $1{,}000^0$C. However, thru our experiments we later determined that the best conditions for annealing our Bridgman grown crystals were in the temperature range of 700^0C to 800^0C. The major focus was to produce gamma ray detection material comparable to CZT, so Brimrose relied more on SRI's past experience to use a fixed partial pressure of 3 to 5 torr (about 0.038 to 0.006 atm). During Phase II we will couple our experimental conditions closely to the defect modeling work.

Several methods of characterization were used to evaluate the level of success achieved with each procedure. Dr. Arnold Burger, a leading expert in the field of material characterization, assisted with characterization activities and evaluation of growth and annealing conditions.

Several detectors were fabricated and processed at Brimrose during Phase I. Various sized crystals were prepared and various detector configurations were used including: planar, pseudo Frish-Grid bar, and pseudo-hemispherical. The devices were read-out on standard single channel NIM-BIN analog MCA electronics at room temperature, initially, at Army Research Laboratory, Adelphi, MD.(POC: Dr. Marc Litz, Phone: 301-394-5556,e-mail: marc.litz@us.army.mil), and later from October 2014 onwards, at Brimrose. The different gamma-ray sources included: Ba-133, Am-241, Cs-137 (this one being the standard source used in nuclear radiation detection field for higher energy gamma radiation) and Co-57. Measurements using Ba-133 source were carried out at ARL. Measurements using Am-241, Cs-137, and Co-57 were carried out at Brimrose. Measurement capability of electron transport properties was also established at Brimrose. The measurement technique was based on the gamma Time-of-Flight (TOF) method, and $\mu\tau$ calculations were based on the well-known Hecht equation, which is described in detail in this report.

In this Phase 1 work, **we have successfully demonstrated the technical feasibility of CdMgTe as a potential gamma-ray detector material.** In fact, not only we were able to demonstrate the gamma spectral response from the CdMgTe detectors grown and fabricated at Brimrose Technology Corporation (BTC) facility, to the best of our knowledge, ***we are also the first to report "spectrometer-grade" gamma detector response from CdMgTe detectors over a wide range of gamma ray radiation, from below 60 keV to above 600 keV.***

Energy resolution in the 3% range has been achieved at 662 keV gamma from Cs-137 source, 6% at 122 keV from Co-57 source and 12% range at 59.6 keV along with lower energy x-ray peaks. All these results have been obtained at room temperature without any additional signal processing correction such as Depth of Interaction (DOI) Correction. **Electron-mobility-lifetime value in our CdMgTe material is about 5.3 x 10^{-3} cm^2/V**

.

These are "ground-breaking" results that can be considered comparable to the existing CZT technology under the same detector size and testing conditions. Specific results and discussions are in section 4 below.

4.0 Results and Discussion

4.1 Crystal Growth

Starting materials

The first thing that is necessary in order to achieve device-grade crystal is that starting materials must be extremely pure (better than 6N, 99.9999%). Commercial elemental Cadmium and Tellurium are available with 7N purity. However, high purity magnesium is *not commercially available* (this is one of the reasons that $Cd_{1-x}Mg_xTe$ has not been extensively considered as a candidate material for gamma-ray detection). Magnesium is only available with 99.98% purity, and is very difficult to purify due to its reactive nature: magnesium burns if heated in the air and rapidly oxidizes under ambient conditions. It burns violently upon contact with water when heated and eventually deteriorates. Hence the purification of magnesium via distillation requires special containers and extremely precise environmental control. (It would be important to note here that pure magnesium is highly reactive and flammable, however upon compounding it to form CdMgTe, it is extremely stable and does not require any special handling procedures and can be handled just like CdTe or CZT)

At Brimrose, we have developed a novel process by which we have successfully purified Mg to the highest level possible. In principle, this is a simple technique which uses volatile nature of magnesium at high temperature. The purification is carried out by the repeated sublimation of magnesium under dynamic vacuum. The salient feature of our purification technique is handling flammable and corrosive (to fused silica container) magnesium in a safe manner without further deteriorating the purity of the starting magnesium material. This novel process is performed in-house [18]. The starting material, Mg of purity 99.98%, either in the form of a solid chunk (D1 in Figure 2) or shavings (D2) was loaded in a specially designed, tapered pyrolitic boron nitride (pBN) crucible (B) which was inserted in silica tubing (A). The assembly was then placed in another silica ampoule (C) with matching inner diameter. A portion of the silica tubing was coated with carbon film.

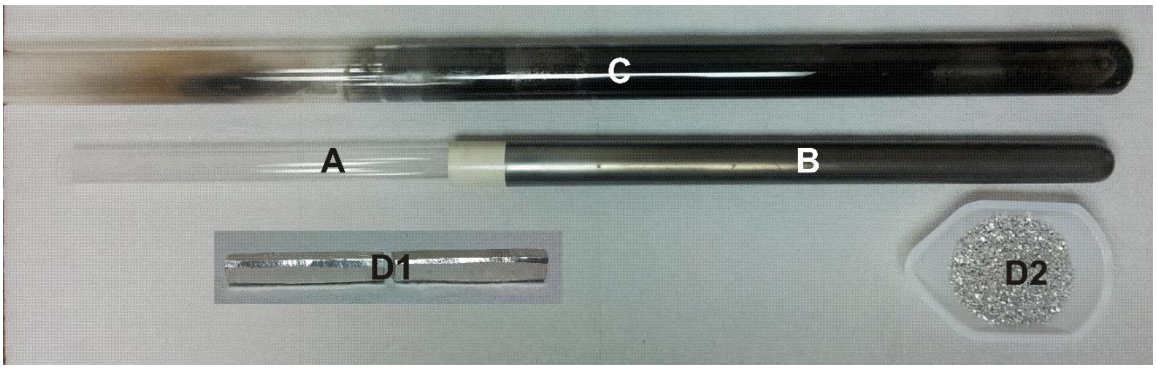

Figure 2. The starting material, Mg of purity 99.98%, either in the form of a solid chunk (D1 or shavings (D2) was loaded in a specially designed, tapered pyrolitic boron nitride (pBN) crucible (B), which was inserted in silica tubing (A). The assembly was then placed in another silica ampoule (C) with matching inner diameter. A portion of the silica tubing was coated with carbon film.

The ampoule was connected to a high vacuum and placed in a furnace. After initial evacuation at lower temperature, the furnace was heated to the temperature gradient shown in Figure 3 and sublimated for about 20 hours, under dynamic vacuum.

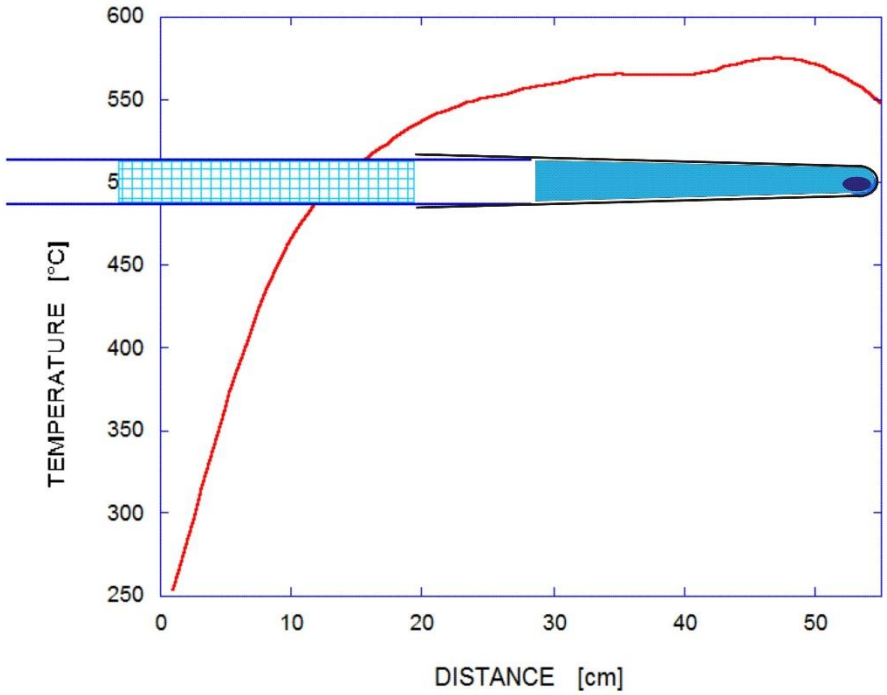

Figure 3. The ampoule was connected to a high vacuum and placed in a furnace. After initial evacuation at lower temperature, the furnace was heated to the temperature gradient and sublimated for about 20 hours, under dynamic vacuum.

After sublimation was complete, the pBN crucible was removed carefully from the ampoule and the sublimed and unsublimed parts were removed as shown in Figure 4. Figure 5 shows the sublimed Mg of improved purity. Figure 5 shows a typical residue found in the crucible and the remaining part of the original (solid) starting material. For most of the Mg deposit, silica can be easily separated exposing a silver shiny material (Figure 6). Figure 6 shows the further purified Mg after resublimation of the material obtained in the first run. This time the left over, unsublimed residue is almost negligible.

Figure 4. After sublimation was complete, the pBN crucible was removed carefully from the ampoule and the sublimed and unsublimed parts were removed

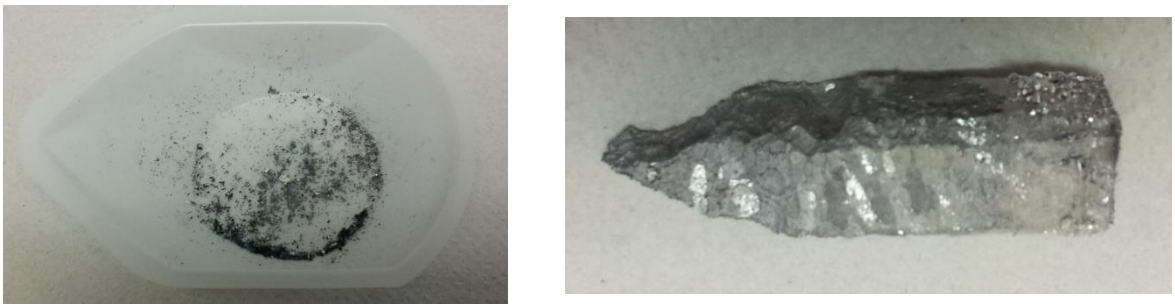

Figure 5. The sublimed Mg of improved purity. Shows a typical residue found in the crucible and the remaining part of the original (solid) starting material.

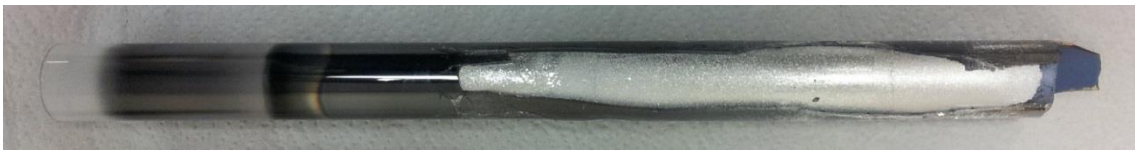

Figure 6. Shows the further purified Mg after resublimation of the material obtained in the first run. This time the left over, unsublimed residue is almost negligible.

The end portions of the resublimed material stuck to the silica glass. The high temperature end of the deposit had a blue tint on the narrow strip of the surface sticking to the glass, and the glass remains were removed relatively easily. At the outer end of the deposit, where the magnesium deposits on the cold end of the tubing, there was a 2-3 cm strip where silica sticks very strongly to the metal (Figure 7).

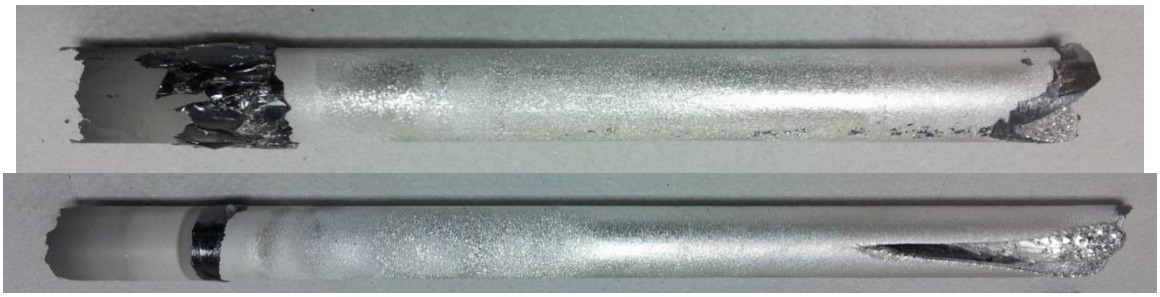

Figure 7. At the outer end of the deposit, where the magnesium deposits on the cold end of the tubing, there was a 2-3 cm strip where silica sticks very strongly to the metal.

Normally we carry out 2 sublimations. If the material has any impurity then it will be indicated by its tendency to stick to the crucible material and the appearance of a blue tinge. With the silica tubing of diameter of 22 mm, the resublimation rate was about 3 g/h. This can be scaled up by using larger diameter crucibles. These crucibles are re-usable after cleaning.

We analyzed our purified Mg by an independent vendor (CMK, s.r.o., Sandricka 30, 96681 Zarnovica, Slovakia). The results of this analysis are shown in Table 1. Material P-Mg24 was obtained from single sublimation of starting 99.98 % pure material D2 in Figure 1 (shavings), while material P-Mg25 was obtained after two sublimations of P-Mg24. Letters F and R indicate the location of the samples (front- hot end, and rear- cooler end of the deposit, respectively).

Table 1. Assay of impurities in purified Magnesium materials after single sublimation (P-Mg24) and double sublimation (P-Mg25).

Element	Sample			
	P-Mg25 F	P-Mg25 R	P-Mg24 F	P-Mg24 R
Li	< 5	< 5	< 5	< 5
Na	< 15	360	< 15	30
Al	120	180	8000	3400
Si	440	7000	9000	11000
P	20	40	400	250
K	< 15	< 15	< 15	< 15
Ca	200	350	1500	300
Mn	330	500	20000	6300
Fe	120	200	9000	2600
Ni	< 5	12	120	32
Cu	300	300	1500	1600
Zn	300	22000	28000	10000
Ga	<=200	<=400	< =400	<=200
Ge	< 300	< 300	< 200	< 200
As	< 30	< 30	< 30	< 30
Sr	< 10	< 10	< 10	< 10
Y	< 5	< 5	< 5	< 5
Zr	< 20	< 20	< 30	< 20
Ag	< 20	< 20	< 20	< 20
In	< 10	< 10	30	< 10
Sn	< 10	35	1200	450
Sb	< 20	< 20	< 20	< 20
Ba	< 20	< 20	< 20	< 20
La	< 5	< 5	< 5	< 5
Ce	< 15	< 15	30	< 15
Gd	< 5	< 5	< 5	< 5
Yb	< 10	< 10	< 10	< 10
Hg	< 20	< 20	< 20	< 20
Tl	< 5	< 5	< 5	< 5
Pb	200	80	5400	2000
Bi	15	45	2000	900
Pu	< 5	< 5	< 5	< 5

Units in the table - ppb weight
RSD (Relative Standard Deviation) is not more than 30%.

We used the material which was sublimed twice and selected the material deposited at the front – hot end of the crucible. This material is has purity of 99.9999%. During Phase II we will go for triple sublimation and have the purity analysis done. Our aim for Phase II is to achieve 7N purity Mg.

Synthesis of Cadmium Magnesium Telluride

The synthesis of Cadmium Magnesium Telluride was conducted in two steps. First, Cadmium Telluride, and then CdTe with high concentration of Magnesium (up to 45%) were synthesized. That two-step procedure was adopted due to high reactivity of magnesium metal with both silica and an alternate synthesis container, pyrolitic Boron Nitride (pBN). Cadmium Telluride was synthesized from a stoichiometric mix of Cadmium and Tellurium pieces loaded into a cleaned and outgassed silica ampoule. The ampoule was evacuated under high vacuum, backfilled with ~0.2 atm high purity Hydrogen, and sealed off. The synthesis was conducted in a tubular horizontal furnace by a gradual increase of (uniform) temperature over a period of a few days up to the temperature of 1000°C, where the material was annealed for at least another week. A single synthesis yielded 300-600 grams of CdTe. The synthesized material was checked for completeness of synthesis and if unreacted elements were found, (which may happen particularly if larger pieces of cadmium were loaded into the ampoule) the coarsely crushed material was annealed for a few hours at 500-600 °C under high vacuum.

The synthesis of Cadmium Magnesium Telluride (high concentration) was conducted in a similar fashion. The differences were in smaller amounts of materials used (not more than 200 grams); smaller size of Mg pieces, and using graphitized ampoules. Despite graphite layer some magnesium pieces that are in contact react with silica. That leads to some loss of magnesium and non-stoichiometry of the telluride and required stoichiometry adjustment as described above for CdTe.

After initial materials studies, the final three $Cd_{.92}Mg_{.08}Te$ crystals doped with Indium and having 0.9 wt% excess Tellurium, were grown in graphitized (carbon coated) thick wall fused silica ampoules by reacting the stoichiometric starting materials directly in the vertical Bridgman furnace. One new technique tried here was: After vacuum sealing the starting material in fused silica ampoule, it was inserted in another graphitized fused silica ampoule with inner diameter about 2 mm larger than the outer diameter of the first ampoule. The first sealed ampoule was then vacuum sealed in the bigger diameter ampoule. This double ampoule arrangement was used to grow the $Cd_{.92}Mg_{.08}Te$ crystals. The preliminary analysis of this material showed better crystal quality and higher resistivity. We will explore this technique in further detail during Phase II.

Doping of CdMgTe crystals requires very small amounts of dopants. For an accurate level of doping, each dopant is dissolved (by melting) in a small amount of CdTe and the ground product of such doped telluride is used for accurate doping of the target crystals.

Crystal Growth

Crystal growth of Cadmium Magnesium Telluride crystals was conducted in pBN crucibles of 22-24 mm in diameter. The crucibles were outgassed and graphitized, as was the ampoule in which the crucible was placed. The crucible was loaded with a desired mixture of CdMgTe and dopants, outgassed under high vacuum overnight, and sealed. The crystal growth took place by Bridgman method in a vertical furnace by translating the ampoule, at a rate of 1 mm/h, from the temperature ~20-30 °C above the melting point thru a temperature gradient.

Figure 8. Shows the typical as-grown and cleaved CdMgTe crystals grown during this Phase I work.

Figure 8. Typical photograph of as-grown and cleaved CdMgTe crystals grown during this work.

One crystal of 25mm diameter was also grown. Larger crystals did not contain significant twins compared to smaller diameter (19 mm) crystals as shown in Figure 9.

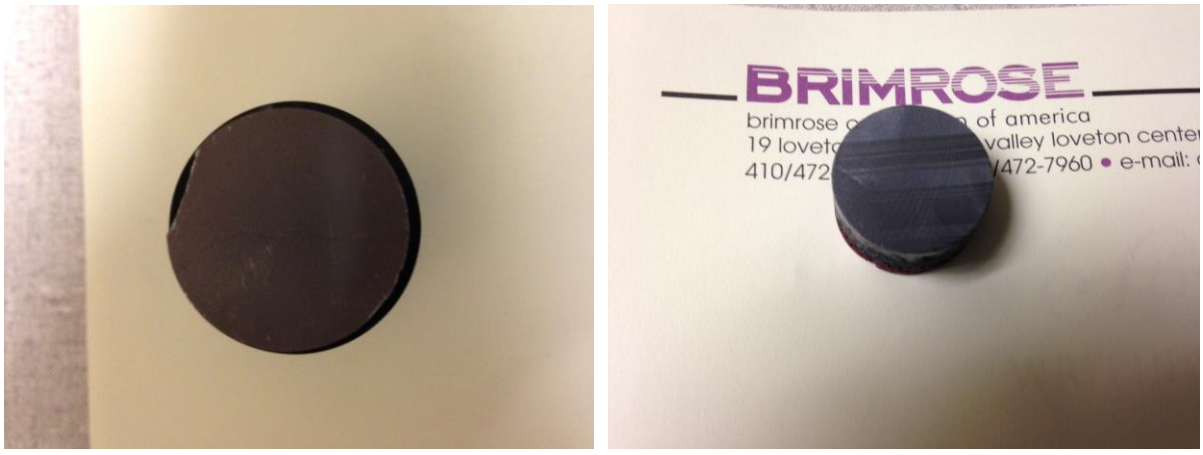

Figure 9. Left Photograph shows lapped cross section of 25 mm diameter Indium doped CdMgTe crystal and the right photograph is that of 19 mm diameter crystal. Left sample is practically twin- free.

During the course of this work, numerous crystals were grown with nominal composition of $Cd_{0.92}Mg_{0.08}Te$. We used the following dopant/dopant combinations:

1) Germanium: Concentration of 1 X 10^{19} atoms/Cm^3;
2) Indium: concentration of 1 X 10^{16} atoms/Cm^3;
3) Indium with 0.8 to 0.9 Wt % excess tellurium: Indium Concentration 5 X 10^{15} to 1 X 10^{16} atoms/Cm^3;
4) Indium and Fe doping Concentrations: 5 X 10^{16} and 10^{15} atoms/Cm^3 respectively;
5) The initial screening parameter we used was resistivity. Material with resistivity lower than 10^8 ohm-cm, were not processed any further. After initial experiments, we determined that only germanium doping and indium doping in concentration range of 5 X 10^{15} to 1 X 10^{16} atoms/Cm^3 with excess tellurium in concentration of 0.8 to 0.9 at% consistently provided high resistivity material (> 10^9 ohm-cm). This material was further explored and most of the good gamma ray quality materials were obtained by growing crystals with these combinations.

These crystals had 65 to 85% single crystalline boules and contained twins. Increasing crystal diameter to one inch and preventing sticking to the crucible wall minimized the number of twins. Dr. Arnold Burger carried out infrared (IR) transmission microscopy on an as-grown germanium doped sample. Figure 10 shows the IR micrograph of a sample, the size of which is indicated on the right hand side in the figure. Figure 11 shows secondary phase distribution in the same sample by size. It indicates that the sample had low volume fraction (10.2 ppm) of average inclusion with average size of 3 μm. Inclusions of this average size and low volume fraction are known to affect less the charge collection, in particular when they are uniformly distributed throughout the bulk.

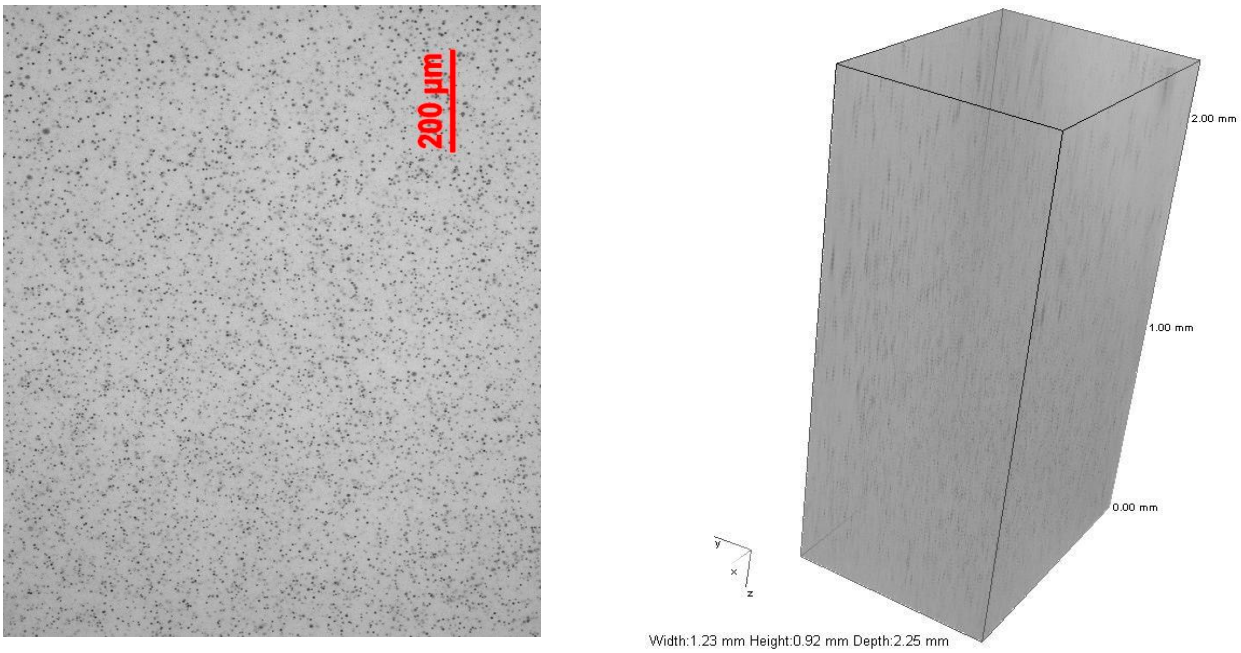

Figure 10. IR transmission microscopy of CdMgTe:Ge sample. Dimensions shown on right.

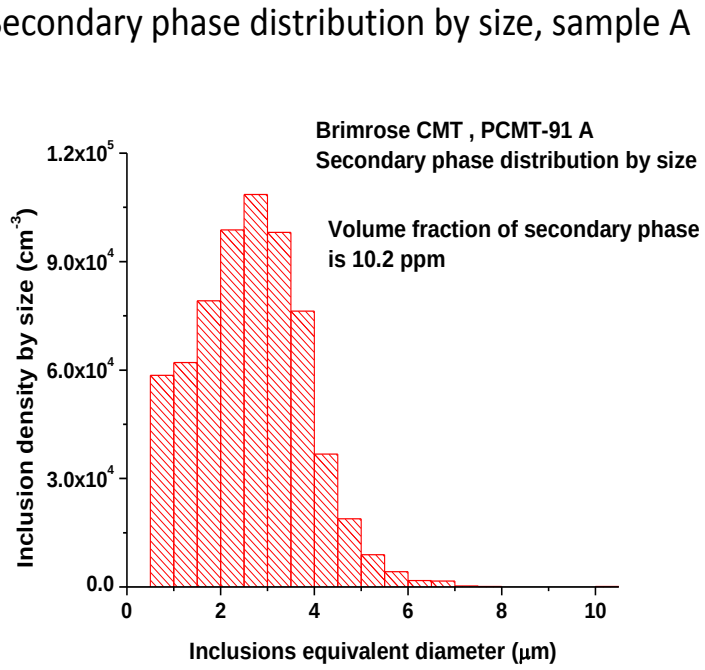

Figure 11. Second phase distribution by size for the CdMgTe:Ge sample shown in Figure 10.

These samples were further processed by annealing them under Cd vapors and subsequently under hydrogen gas which will improve them further. This improvement was demonstrated by actually fabricating the gamma ray detectors and measuring their I-V characteristics.

In order to achieve our goals in a timely fashion we had screened and further characterized the crystal samples displaying high resistivity and high sensitivity to ambient light (photo-conductivity) by fabricating gamma ray detectors from them. The gamma ray response and I-V characteristics of these materials were measured to qualify these crystals. This work is described in the section 4.3 on CdMgTe Detector Work and Discussion of Results.

Annealing Conditions

Samples were cut and prepared from the crystals that were grown as described above. The samples were then cleaned in Alconox detergent solution, and then in organic solvents using an ultrasonic bath. For annealing, the samples were loaded in a 15 to 19 mm inner diameter quartz ampoule and vacuum sealed with 70 to 100 mg, high purity (6N) cadmium pieces. This amount of cadmium provided an over-pressure of cadmium vapors. The length of the sealed-off ampoule was about 10 to 12 cm.

Figure 12 shows the crystal samples sealed in a specially designed ampoule at Brimrose for annealing work. This is the usual technique at Brimrose for the annealing process. If we need the annealing under known controlled pressure then we carefully determine the volume of the ampoule after it will be sealed and use a carefully weighed amount of Cd pieces necessary to provide required partial pressure. The weight of required Cd is determined using the gas-law equation PV=nRT where P is pressure, V is the ampoule volume, n is the mole concentration of Cd, R is the gas constant and T is the processing temperature.

Figure 12: Photograph of a typical annealing ampoule used at Brimrose. CdMgTe samples are vacuum sealed in the specially designed ampoule. Small Bulb on left hand side contains pieces of high purity Cadmium.

Samples were annealed in a horizontal furnace with an isothermal profile at a temperature range of 750 to 800 ^{o}C, for 3 to 5 days, depending upon the thickness of samples.

During Phase I, the focus was on obtaining the detector grade material. Therefore, experiments under various controlled partial pressure of Cd vapors were not carried out. Annealing of all the samples were carried out under Cd over pressure in the range 3 to 5 torr (3.9×10^{-3} to 6.6×10^{-3} atmospheres). This pressure prevented loss of sample material being annealed via sublimation. In

Phase II we will systematically couple other data points (partial pressures) used in defect modeling by SRI.

Several samples were also annealed under H2 gas atmosphere after Cd annealing, under the same temperature conditions. The samples with the best gamma response were obtained with both Cd and H2 gas annealing. This processing method was developed during the last month of this STTR program hence SRI did not have adequate time to develop the code for H2 annealing. SRI will address this during phase II.

It is known that the best current gamma ray detector (mostly CZT) in the field have been produced only after post processing. Our goal in Phase II, by tightly coupling our experiments with SRI's defect modeling, will be to explore the possibility of in-situ processing of gamma ray detector material or develop a low-cost, reproducible, post-processing, batch method, similar to that used in silicon technology.

4.2 Modelling Work

The objective of this study was to develop strategies to obtain high resistivity and high-$\mu\tau$ product CdMgTe for gamma-ray detector application. The modeling work was performed at SRI International (SRI).

The resistivity, mobility, and lifetime are all strongly impacted by the presence of defects in the material. Although extended defects such as dislocations and stacking faults can be minimized during crystal growth, native point defects (such as interstitials, vacancies, and antisites) will always be present in as-grown crystals. The density of each class of defect is determined by the thermodynamic conditions during growth, such as the temperature at the growth front and the chemical potentials of the constituents in the liquid from which the crystal is being grown. If a defect has ionization states, the density of each defect will also depend on the Fermi level during equilibration. The native defects – and therefore their detrimental contribution to the carrier lifetimes – can be manipulated through control of one or more of the following:

- Growth conditions (temperature and stoichiometry);
- Intentional addition of dopants and/or deep-level impurities (specific atom(s) and their densities); and
- Post-growth anneal (temperature and cation partial pressure).

<u>Code Development</u>

In this project, SRI developed a MatLab code to calculate the defect concentrations in a crystalline material using the generalized quasi-chemical approximation. The approach has been discussed extensively in the literature (Kroger 1964 [19]) and was extended and applied to semiconductor defect analysis in HgCdTe and CdTe by Berding (Berding *et al.* 1994 [20], Berding 1999 [21]. The code developed in Matlab follows the approach outlined in Berding *et al* (1994) [20]. The MatLab code developed will calculate:

- Equilibrium defect concentrations as a function of temperature and cadmium partial pressure;
- Defect re-equilibration upon quenching from equilibration temperature to lower temperature with total defect concentrations frozen (due to limited diffusion at the lower temperatures), but with the fraction of ionized defects allowed to change in response to the lower temperature;
- Both equilibration and quenching results for material with an arbitrary density of shallow or deep donors or acceptors;
- The Fermi level and the resulting electron and hole densities both during equilibration and upon quenching.

The input for the code includes:

- Materials properties
    - Defect formation energies for any number of defects (calculated using *ab initio* methods such as those based on the local density approximation (LDA);
    - Defect formation vibrational enthalpy and entropy;
    - Ionization energy levels in the band gap associated with the defect (single or doubly ionized donor or acceptor level);
    - Electron and hole effective mass for the calculation of the electron and hole densities;
    - Temperature-dependent band gap for calculation of ionization states and Fermi level.
- Impurity and dopant properties
    - Concentration (acceptor or donor) and ionization levels of intentionally introduced impurities in the lattice.
- Equilibration conditions (*e.g.* growth conditions or anneal conditions)
    - Temperature at which defects are assumed to form and equilibration with each other;
    - Partial pressure of the cationic species, the cadmium partial pressure for CdMgTe.
- Quench temperature
    - Temperature of interest ("quench temperature"). It is assumed that the defects are formed under the equilibration conditions, but at that which the free carriers (electrons and holes) can re-equilibrate at the quench temperature and the total concentration of defects is frozen in (e.g., at the equilibration conditions, one might have a concentration of neutral and ionized cadmium vacancies of $[V_{Cd}^{0}]$ and $[V_{Cd}^{-1}]$; t the quench temperature, $[V_{Cd}^{0}] + [V_{Cd}^{-1}]$ is unchanged, but the ratio $[V_{Cd}^{-1}]/ [V_{Cd}^{0}]$ will in general change.

Inputs for CdMgTe

For the current program, we are using the defect formation energies calculated previously; in future programs, these energies will be updated, calculated using larger super cells (i.e., with higher accuracy), and should include the Mg-related defects such as the Mg interstitials and the Mg antisite (Mg_{Te}). Such calculations are beyond the scope of the current effort. Because Mg is in low concentration in the present study (~ 10%), we expect the error associated with ignoring

the Mg-related defects to be relatively small. The defect formation energies and entropy were taken from Berding (1999) [21].

We assumed that the effective masses for CdMgTe were approximately the same as those of CdTe. The calculations also require the temperature-dependent band gap in the materials for the calculation of the defect densities when they form at the high growth temperature, as well as their re-equilibration upon cooling. While the composition-dependent band gap of CdMgTe at room temperature appears to be well documented, we have not yet found the temperature-dependent band gap. As such, we have assumed the same temperature dependence as the band gap of CdTe, which we believe should be a good approximation.

Because the bounds for CdMgTe were not found, for equilibration conditions we used the bounds of the P-T existence region for CdTe and 10% CdZnTe as guidance. Because of this uncertainty, the Cd-saturated and Te-saturated bounds may be in some error. This should be kept in mind when interpreting the results.

Results of Modelling Work

We explored a range of equilibration conditions using this code. In Figure 13, we show the results of material annealed with no impurities added. These results are for CdMgTe with 10% Mg. The notation is as follows: V_{Cd} is the cadmium vacancy, Te_{Cd} is the tellurium antisite, V_{Cd}-Te_{Cd} is the cadmium vacancy-tellurium antisite complex, and Cd_I is the cadmium interstitials. Because the density of the tellurium vacancy, the cadmium antisite and the tellurium interstitial did not impact the results shown here; they are not included in these plots. Note that the total concentration of each defect is plotted, which is the sum of the neutral and all of the ionized states of that defect. As noted above, the assumption is that the total number of defects does not change upon quenching, only the fraction ionized. The electron and hole carrier densities are shown both at the equilibration temperature and at room temperature. Also shown are the conduction and Fermi level, where the valance band edge is taken as the zero of energy.

Note a few things about these results. At the equilibration temperatures, the material is nearly intrinsic for almost the complete range of stoichiometry. At room temperature and at low cadmium partial pressures, the material is *p*-type, due to the high density of cadmium vacancies. At room temperature and under high cadmium partial pressures, the materials is *n*-type due to a high cadmium interstitial density. There is a narrow region of intrinsic behavior (with carrier concentrations $< 10^{10}$ cm^{-3}), where the resistivity might be suitable for gamma-ray detectors. To access this region, the material would have to be annealed at the partial pressure corresponding to the intrinsic region (*e.g.*, ~ 1 atm at 900 °C), then quenched to room temperature. This approach is not feasible for a number of reasons. First, the partial region over which the carrier concentration is low is quite narrow, and it would be difficult to control the temperature and pressure conditions precisely enough to access this region. Second, the modeling shown here is accurate to determine overall properties, but the exact location of the low-concentration region is not likely accurately predicted, due to even small errors in the calculations. Finally, any unintentional impurities could shift the position of this region.

In Figure 14, we show similar results, but this time for the equilibration at 1000°C and 700°C with shallow donors present. An ionization energy of 0.015 eV was assumed, approximately the ionization energy in indium in CdZnTe. The overall behavior is similar at 1000°C and 700°C. There are a few things to note about these results. As the donor concentration increases, the region of intrinsic behavior broadens. At low donor concentration, there is insignificant

compensation of the cadmium vacancies that dominate the p-type carrier behavior that is present through most of the existence region. As the concentration of the donor increases, significant compensation can occur over some ranges of partial pressures, as can be seen in Figure 14(c) and 14(f). As in the case of the undoped material, these results suggest that donor doping to achieve highly intrinsic material is not a robust approach for similar reasons. Yet experimentally it has been found the n-type doping can produce intrinsic material. The only way to reconcile that finding with the present work is by considering some defect relaxation or complexing mechanism.

In Figure 15, we show results for material equilibration at 1000^{o}C and 700^{o}C with mid-gap donors present. Here the behavior is quite different. We see that, in all cases, the intrinsic region is relatively wide, and for 10^{17} cmd^{-3} mid-gap donors, the material is intrinsic throughout the complete stoichiometric region both at 1000^{o}C and 700^{o}C. This observation of high resistivity material with mid-gap states has been well documented in the literature, and this result is consistent with those findings.

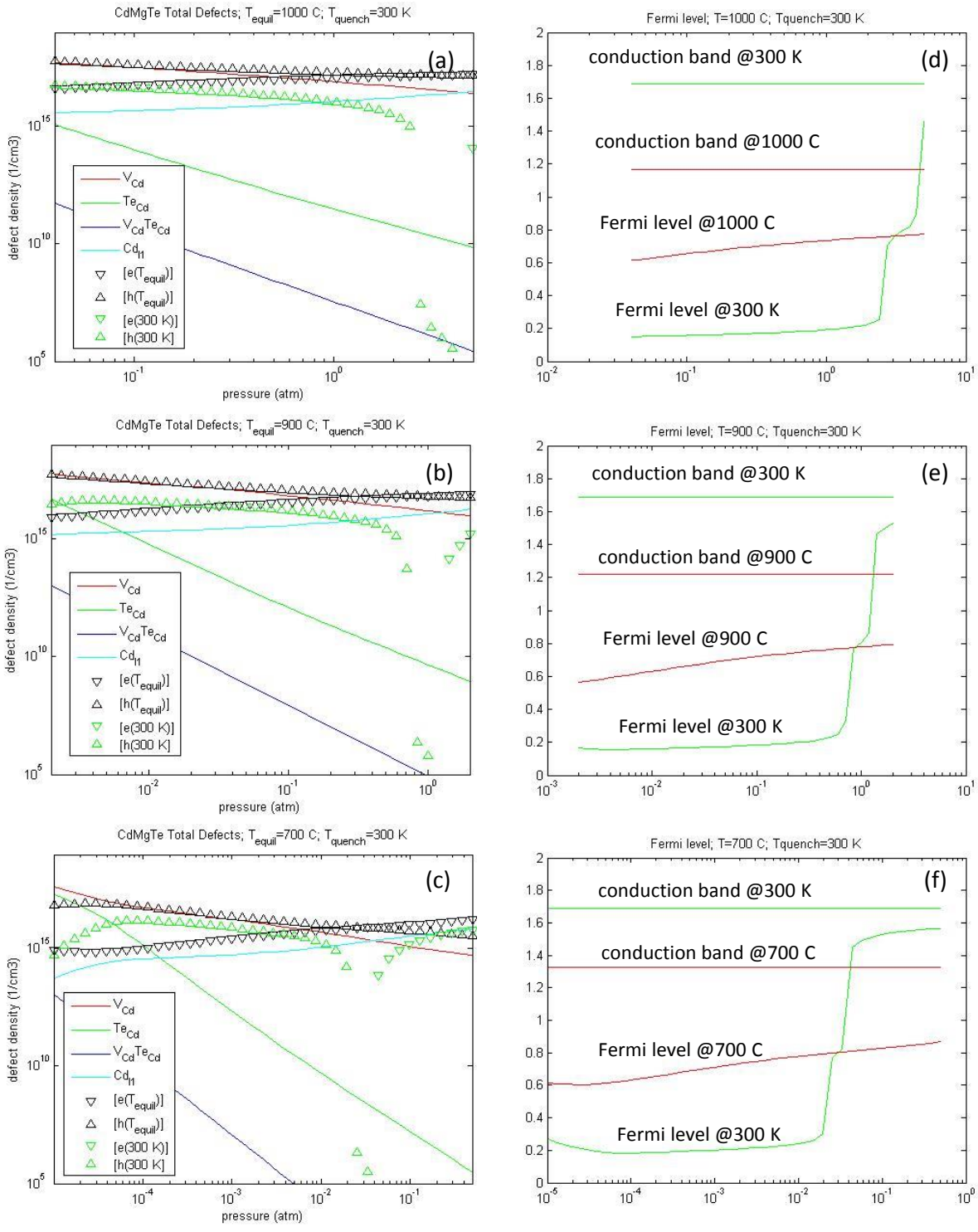

Figure 13. Total defect concentrations at (a) 1000^{o}C, (b) 900^{o}C, and (c) 700^{o}C, and the corresponding band gap and Fermi levels (d), (e), and (f).

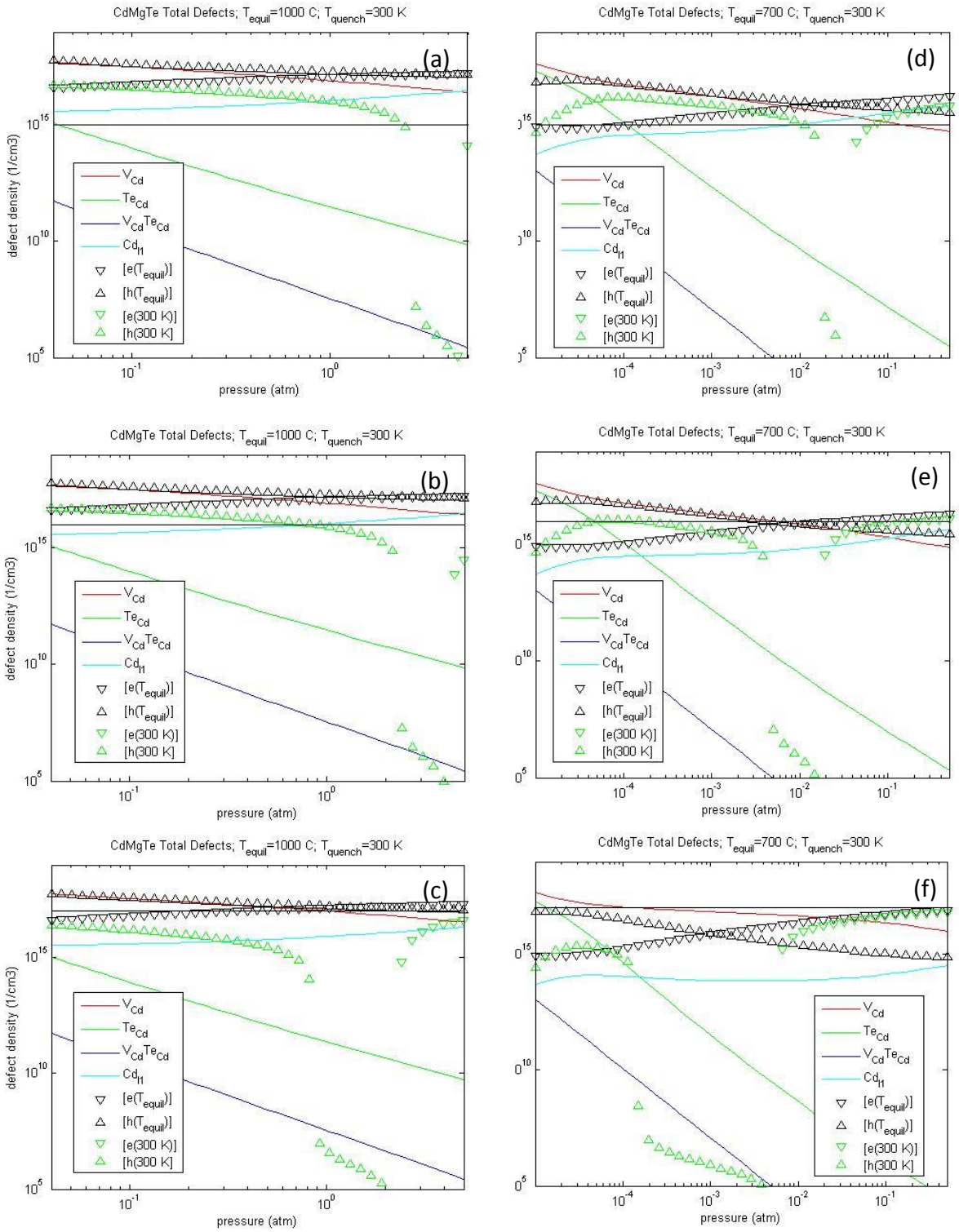

Figure 14. Total defect concentrations at (a, b, c) 1000°C, and (d, e, f) 700°C, for material with: (a) and (d) 10^{15} cm^{-3}; (b) and (e) 10^{16} cm^{-3}; (c) and (f) 10^{17} cm^{-3} shallow donors.

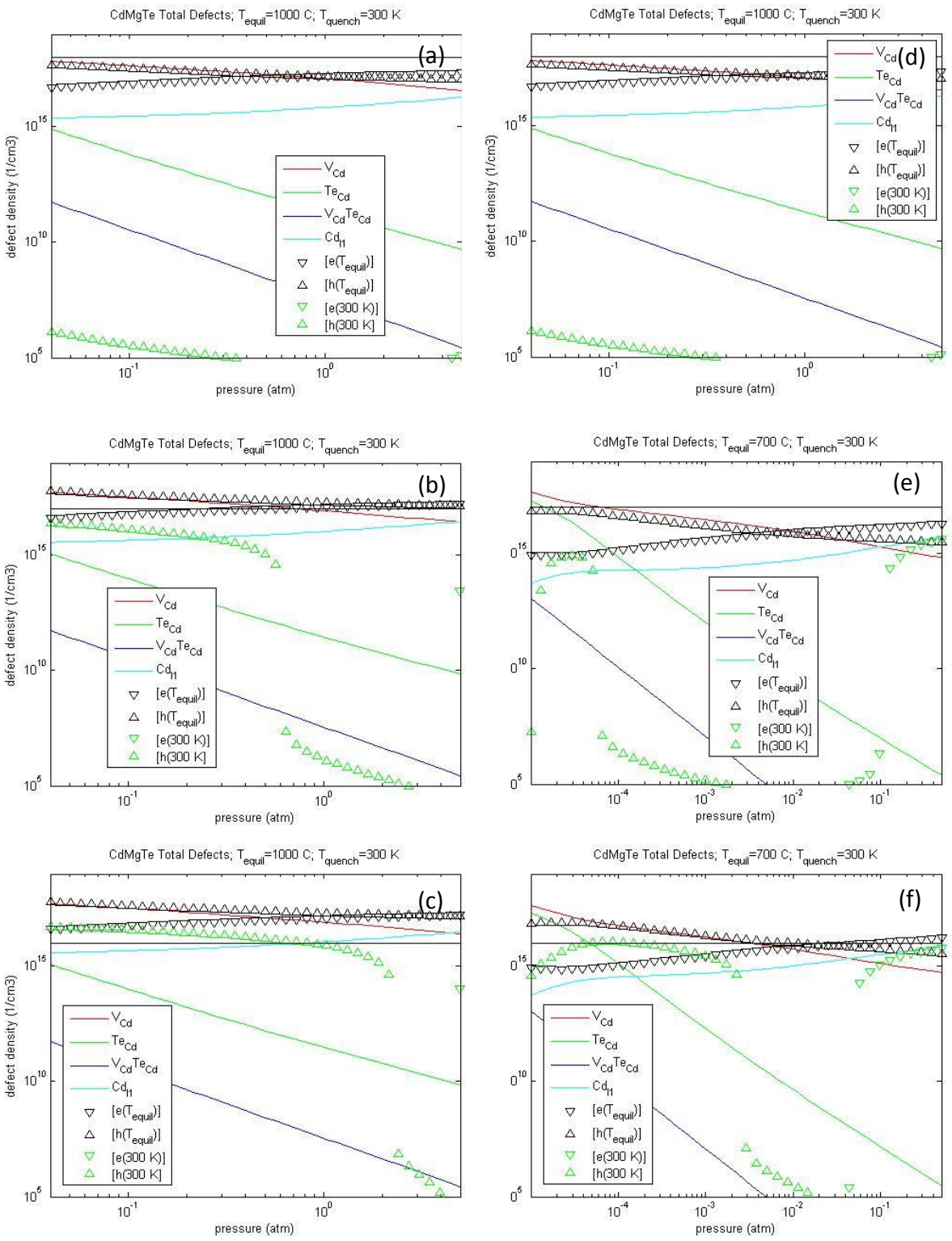

Figure 15. Total defect concentrations at (a, b, c) 1000 ^{o}C, and (d, e, f) 700 ^{o}C, for material with: (a) and (d) 10^{16} cm^{-3}; (b) and (e) 10^{17} cm^{-3}; (c) and (f) 10^{18} cm^{-3} mid-gap donors

In conclusion, indium doping was predicted to produce intrinsic material for a range of equilibration conditions. It was found that as the indium concentration increased, the region of intrinsic behavior broadens. At low indium concentration, there is insignificant compensation of the cadmium vacancies that dominate the p-type carrier behavior that is present through most of the existence region. As the concentration of the donor increases, significant compensation occurs over a broad range of partial pressures.

The modeling predicts that highly intrinsic material can only be achieved by relatively careful control of the cadmium partial pressure, which needs close coupling with experimental conditions for more accurate verification of the current model. The detailed understanding might need the consideration of defect relaxation or complexing mechanism that was not considered in the present work, but will be explored in subsequent projects.

Now that Brimrose has a bench mark conditions for producing gamma ray quality CdMgTe material, this will be used as a starting point of subsequent modeling. The phase II work will allow more mutual feedback between experimental and modeling work to build up more robust code and defect models.

4.3 CdMgTe Detector Work and Discussion of Results

Gamma ray detectors from the $Cd_{(1-X)}$ $Mg_{(x)}$ Te crystals that we prepared were fabricated and processed at Brimrose. The devices were read-out on standard single channel NIM-BIN analog MCA electronics at room temperature, initially, at Army Research Laboratory, Adelphi, MD.(Point Of Contact: Dr. Marc Litz, Phone: 301-394-5556,e-mail: marc.litz@us.army.mil), and later from October 2014 onwards, at Brimrose (See Figure 16). The different gamma-ray sources included: Ba-133, Am-241, Cs-137 (this one being the standard source used in nuclear radiation detection field for higher energy gamma radiation) and Co-57. Measurements using Ba-133 source were carried out at ARL. Measurements using Am-241, Cs-137, and Co-57 were carried out at Brimrose. Measurement capability of electron transport properties was also established at Brimrose. The measurement technique was based on the gamma Time-of-Flight (TOF) method, and $\mu\tau$ calculations were based on the well-known Hecht equation, which is described in detail in this report.

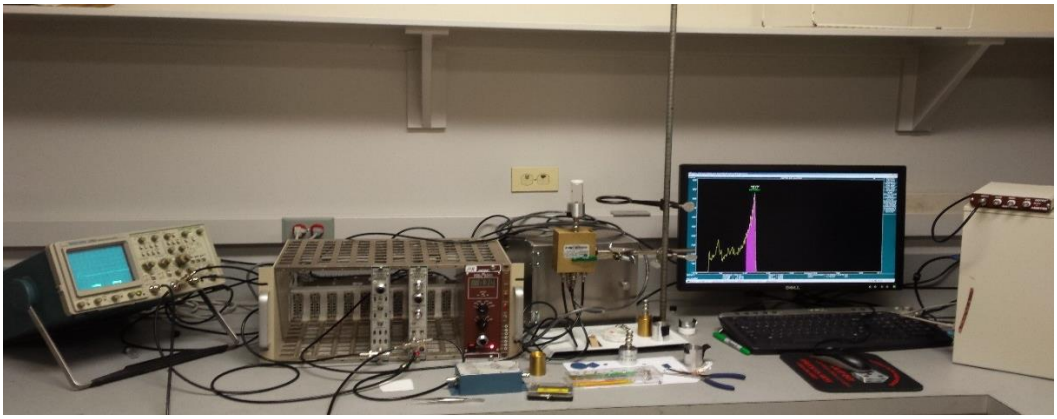

Figure 16. Standard NIM-BIN MCA system for nuclear spectroscopy measurement at BTC.

We report here our continuous progress and success in the demonstration of gamma spectral response from CdMgTe detectors.

In a September we obtained our first detector results measured at the Army Research Lab in Adelphi, MD. We were able to detect both 81 keV and 356 keV gammas from Ba-133 source. The measurements have been achieved in a few different samples, in two different configurations. All of the devices in this report were read out on standard single channel NIM-BIN analog MCA electronics at room temperature. The irradiation is from a 3mm dia. source placed very close to the detector housing entrance.

(a) 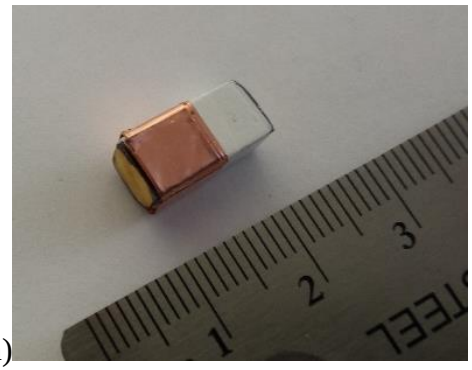 (b) 

Figure 17. CdMgTe detectors grown and fabricated at Brimrose: (a) A 5x5x12.5 mm^3 Pseudo Frisch-Grid bar shape detector, (b) A 9x12x9 mm^3 Pseudo-hemispherical configuration detector.

Shown in Figure 18 is the Ba-133 gamma response of the 5x5x12.5 mm^3 CdMgTe detector (Figure 17a) in Pseudo Frisch-Grid bar shape configuration, where both the 356 keV and the 81 keV gammas can be seen and well resolved with measurable Full-Width-at-Half-Max (FWHM) value. Figure 19 shows the 81 keV response of another BTC CdMgTe detector, 9x12x9 mm^3, in Pseudo-hemispherical configuration (Figure 17b).

These initial results were very encouraging since they demonstrated the feasibility of our CdMgTe as a gamma ray detector material.

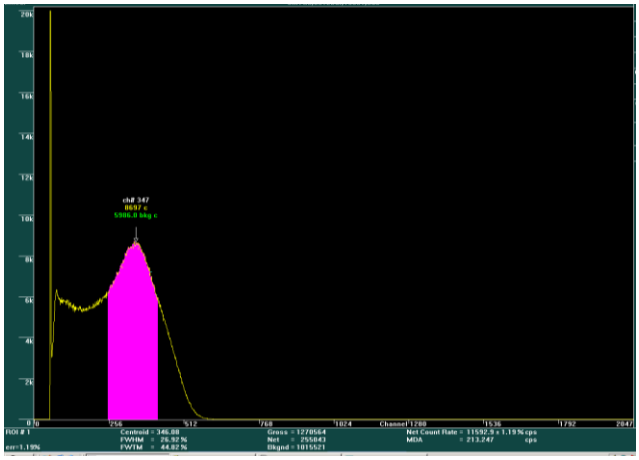

Figure 18. Ba-133 gammas response of a Brimrose 5x5x12.5 mm^3 CdMgTe detector shown in Figure 17a showing both 356 keV and the 81 keV gamma response.

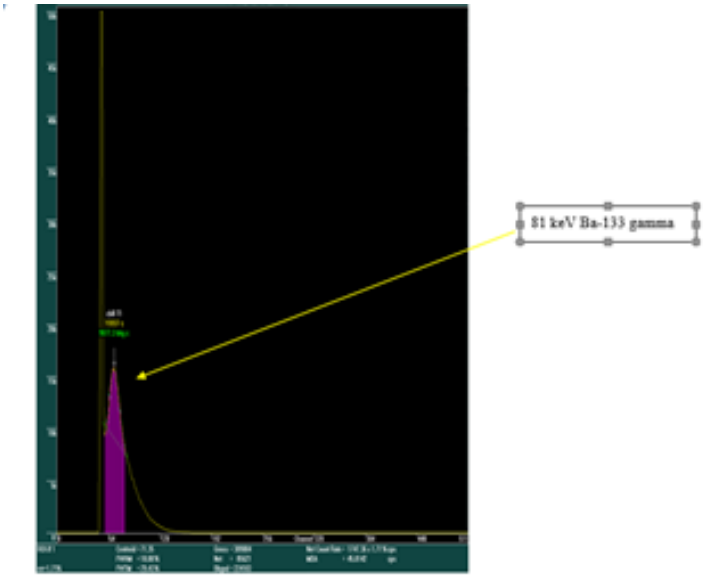

Figure 19. Ba-133 81 keV response of a Brimrose 9x12x9 mm^3 pseudo-hemispherical CdMgTe detector (shown in Figure 17b).

We also measured in October 2014, the Cs-137 662 keV response of another thinner sample, 6x9x2 mm^3 detector with 2 small circular electrode pair, ~ 2.5 mm diameter on each planar side (cathode and anode). However, despite the 662keV energy resolution obtained on that sample, the Compton edge was not seen and efficiency was obviously low from a sample with just 2mm thickness for 662 keV gamma. We therefore decided to prepare other much thicker samples to properly measure the 662 keV responses while continuing to optimize the crystal growth and post-growth processing conditions.

Significantly better results were subsequently achieved on a 10mm-thick sample. These results were measured at Brimrose when we had established the full in-house capability to measure

gamma response. Again, measurements were performed via standard single channel NIM-BIN analog MCA electronics.) Figures 20-23 show the 662 keV gamma responses from a 4x4x10 mm^3 Pseudo Frisch-Grid CdMgTe detector where energy resolution of 3.4% (FWHM) was achieved at room temperature without any additional signal correction. ***This is a "ground-breaking" result that is considered comparable to existing CdZnTe (CZT) technology using the same detector size and testing conditions.***

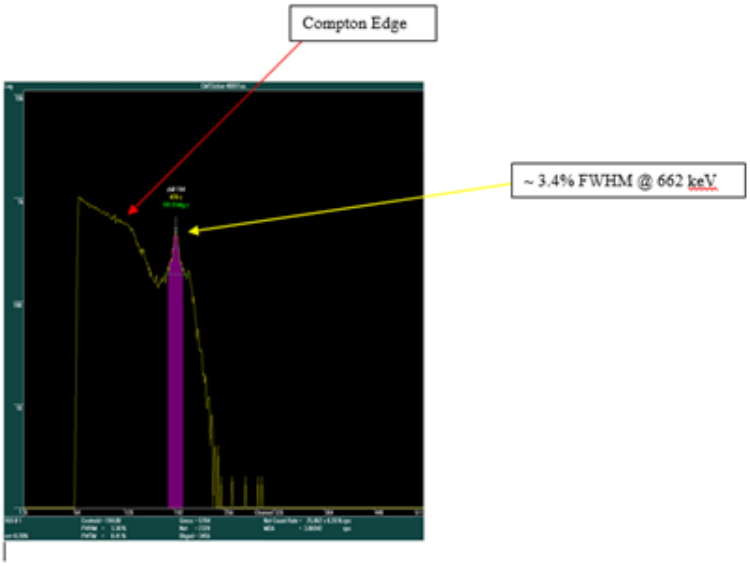

Figure 20. Log plot of BTC CdMgTe 4x4x10 mm^3 Frisch-Grid bar detector Cs137 gamma response at 400V, 1us peaking time, no collimation, room temperature, no additional signal correction/processing.

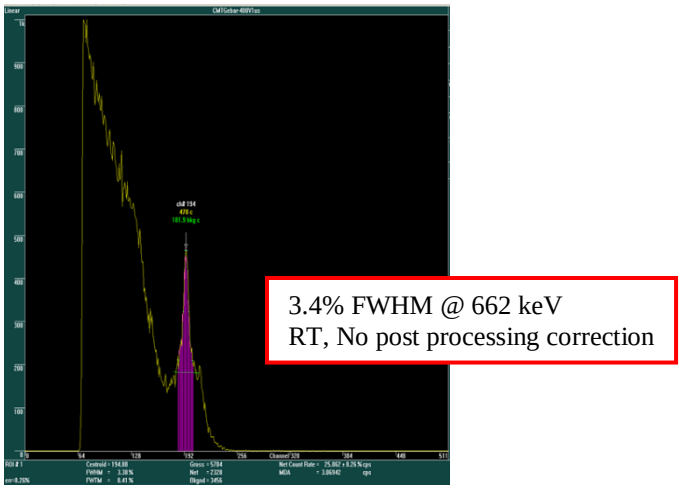

Figure 21. Linear plot of the very same 10mm-thick CdMgTe detector shown in Figure 20, also at 400V.

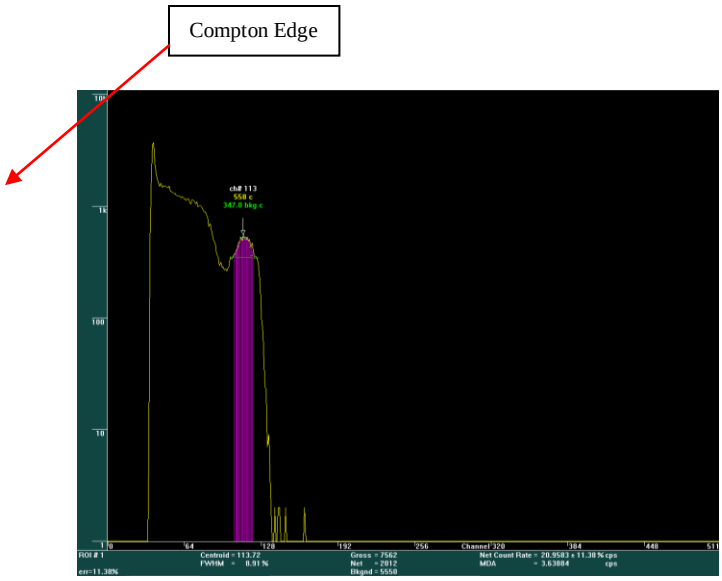

Figure 22. 662 keV gamma response of the same 10mm-thick detector @ 500V, log plot.

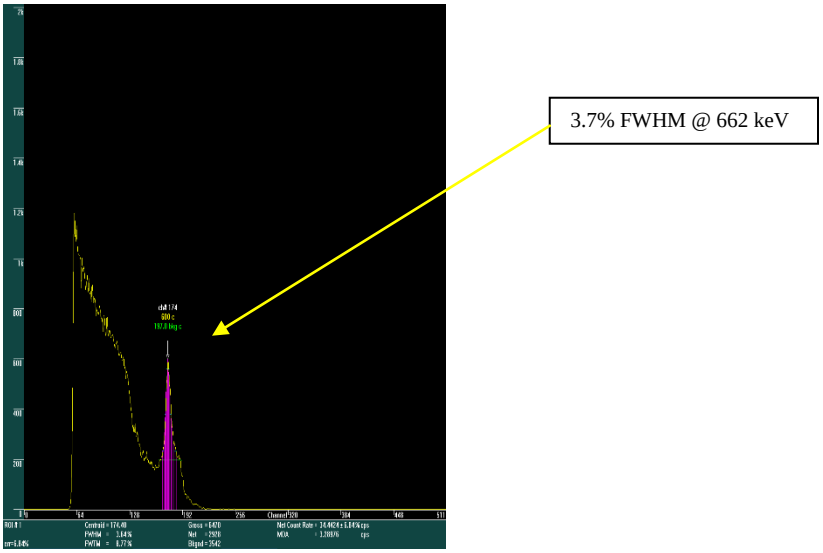

Figure 23. 662 keV gamma response of the same 10mm-thick detector @ 350V, linear plot.

Note that an "uncorrected" 3% energy resolution @ 662 keV is a very encouraging result for the wide band-gap room temperature semiconductor detector (RTSD) community since CdMgTe has been predicted theoretically to have the potential to be as good if not better than that of CdTe and CZT. **This level of "spectrometer grade" higher energy gamma detector performance can only be possible when the material has excellent charge-transport properties, which is indicated by the lower energy gamma response when measured in thinner form.**

To verify this theoretical basis, we prepared a thinner sample from the very same material that exhibited the 662 keV response shown in Figures 20-23 by cutting out a ~2 mm-thick sample from the 4x4x10 mm3 sample and tested the planar 4x4x2 mm3 with Am-241 59.6keV gamma

source. The result is very consistent and as expected. Figure 24 shows the Am-241 gamma response of this 4x4x2 mm3 planar CdMgTe detector where an energy resolution of 12.8% @ 59.6 keV gamma has been achieved. What is special is that other much lower energy x-rays peaks and escape peaks can also be well detected and resolved. Note that even at 10mm-thick, the detector such as that used for the measurements in Figures 20-23, can still respond well to Am-241 lower energy gamma (Figure 25).

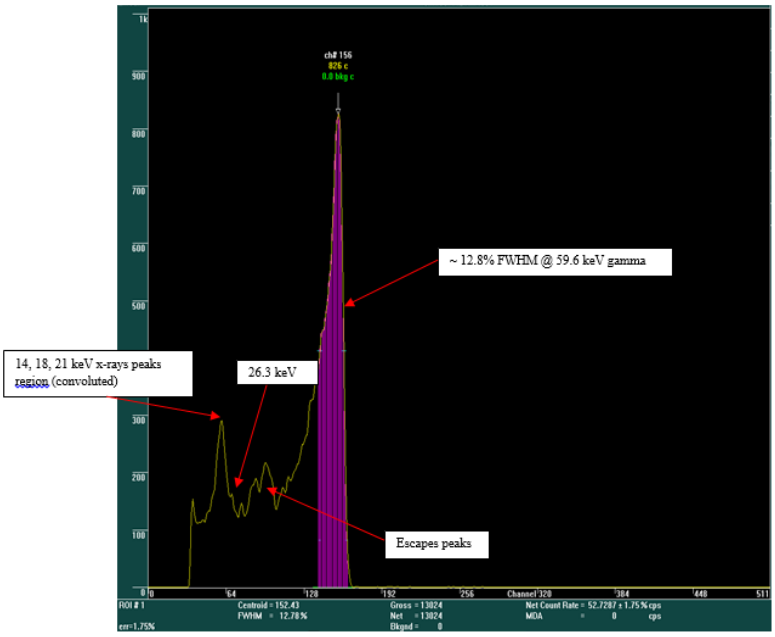

Figure 24. Am-241 response of a BTC 4x4x2 mm3 planar CdMgTe detector.

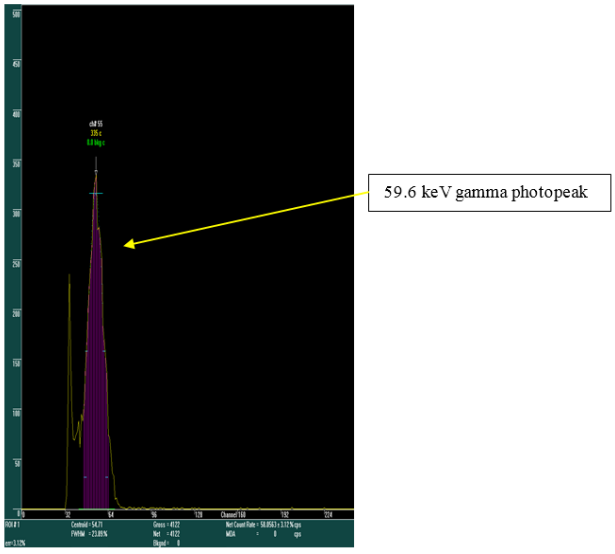

Figure 25. Lower energy gamma response of a BTC 10mm-thick CdMgTe detector.

Since the CdMgTe detector responded well to gamma energy < 60keV (via Am-241 source) and higher energy gamma > 600 keV (as with Cs-137 source), we expected that it would also respond well to medium energy gamma such as 122 keV of Co-57, a common gamma source used heavily to test CZT detectors, (especially for medical imaging applications for instance.) Our most recent characterization showed just that – Using the very same material from the 4x4x10 mm3 and 4x4x2 mm3 sample just mentioned, **we obtained "spectrometer grade" Co-57 response on the resulting 4x4x6 mm3 sample (Figure 26).** The 6 mm thickness will stop the majority of the 122 keV gamma from this source. Note that the pulser width (3.1%) indicates the electronic noise of the system, and hence the intrinsic resolution of the detector, should also be in the 3% range theoretically rather than the 6.7% as measured, as can be seen from Figure 26.

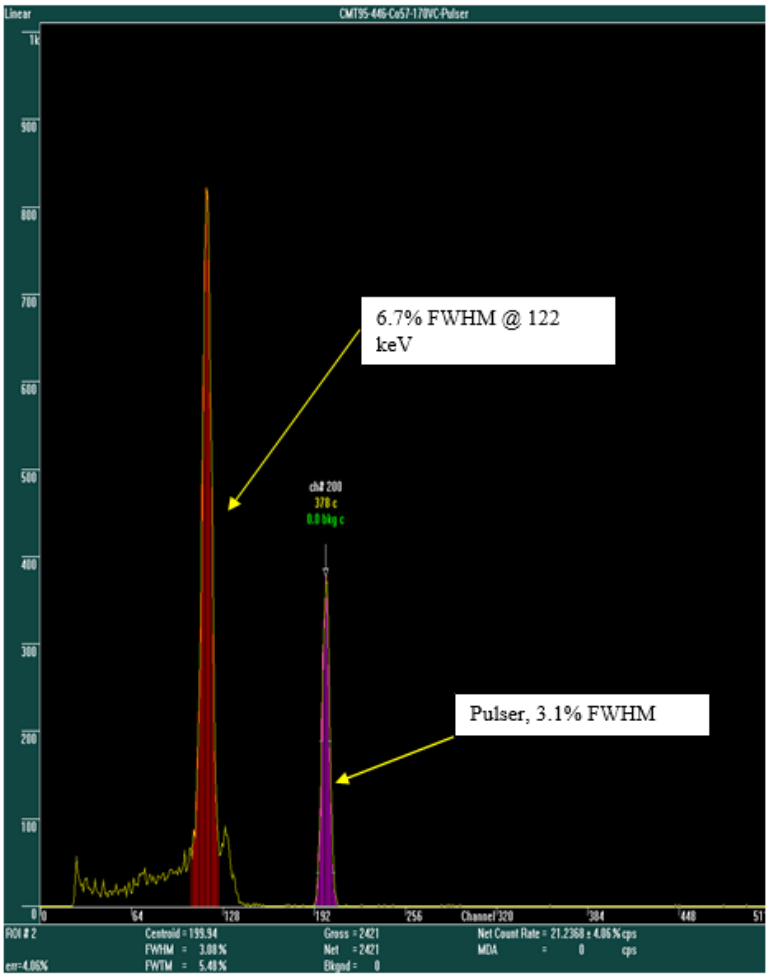

Figure 26. BTC's 4x4x6 mm3 Pseudo Frisch-Grid CdMgTe detector with collimated Co-57 gamma response, 170V bias, RT, no signal correction.

Furthermore, **great detector performance usually goes hand-in-hand with good electrical transport properties of the material, especially the mobility-lifetime (mu-tau) of the main**

carrier, electrons. We therefore went a step further, establishing electron-mu-tau measurement capability in-house via the Gamma Time-of-Flight (TOF) method via Am-241 gamma source, based on the well-known Hecht equation (Figure 27). The result: **extracted electron mobility-lifetime (μτ) value in our CdMgTe material was 5.3 x 10^{-3} cm^2/V, *a consistent "high mu-tau" result very comparable to that obtained with spectrometer grade CZT (which represents existing technology).*** Note that this is the number one figure of merit for compound semiconductor–based radiation detector as we mentioned from the beginning of this report.

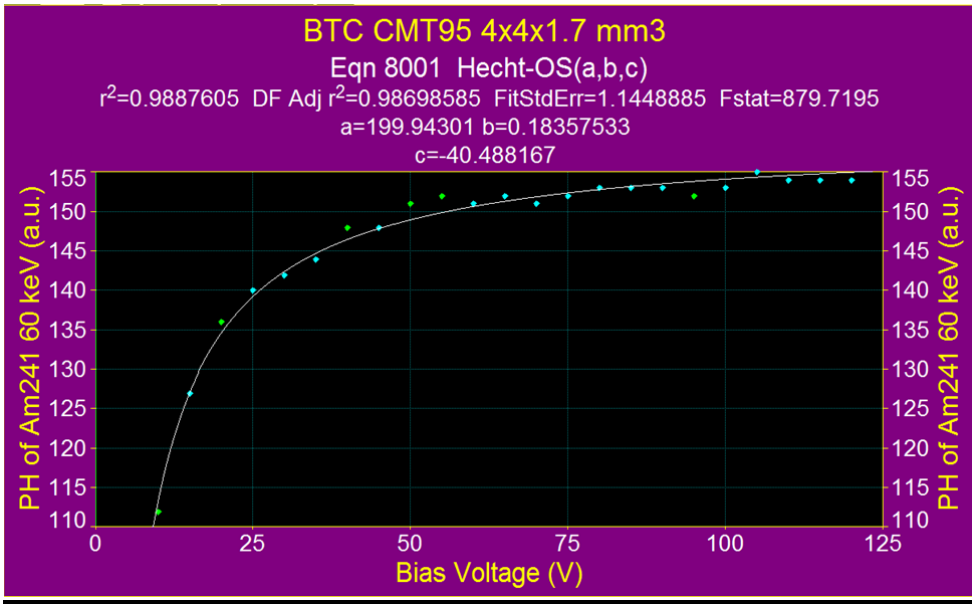

Figure 27. Curve fitting of the Am-241 gamma response of BTC's CdMgTe detector from which a value of 5.3 x 10^{-3} cm2/V was obtained for mu-tau-electron.

Discussion of Results

The results from Figs. 14 to 21 can be attributed to either: (1) the material properties or (2) the device design, fabrication and electronic instrumentation.

(1) The role of material qualities:

First, material qualities and properties play a deterministic role in the detector's performance. It is critical to point out that the samples used to obtain the reported results (Figs. 20-26), all have a proprietary material purification and crystal growth process (including a special doping recipe -**all In-doped in this case**) but also have special post-growth annealing treatment as well.

Proper doping is critical in achieving the proper electrical compensation needed to obtain high resistivity and especially good electrical transport properties (See Fiederle et.al. Ref [20] for instance). Prior to obtaining our current best growth recipe where bulk resistance is always much higher than 10^9 Ohm, bulk resistances measured can be much lower when different doping concentrations were used. Even the type of dopant can make a huge difference as evidenced by the differences between our In-doped and Ge-doped samples.

Figure 28 shows examples of the IV measurements of our (a) In-doped CdMgTe sample vs that of (b) Ge-doped CdMgTe sample where the device resistivities are 3.12 x 10^{10} ohm-cm and 1.44 x 10^{9} ohm-cm respectively. The bulk resistivities were extracted from the -5V to +5V IV curve region for the In-doped sample and from -2V to +2 V region for the Ge-doped sample. They are 1.64 x 10^{10} ohm-cm and 1.8 x 10^{9} ohm-cm also respectively.

(a) 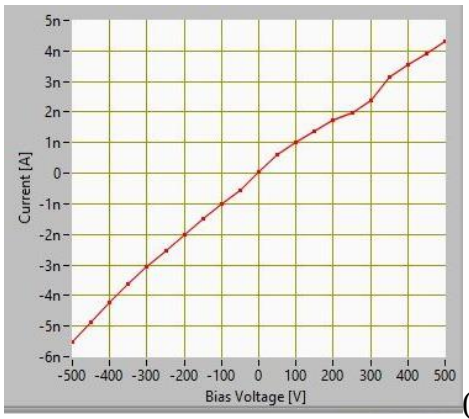

(b) 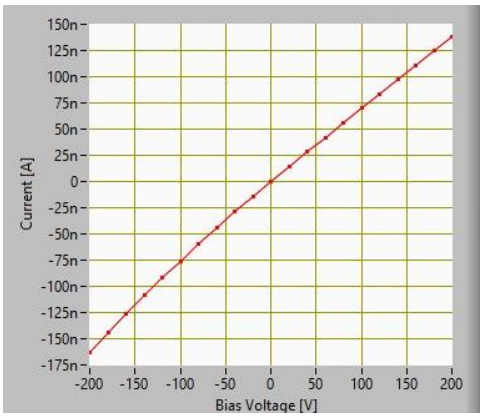

Figure 28. IV measurements of BTC's CdMgTe detectors where resistivities have been obtained: (a), an In-doped 4x4x6 mm3 CdMgTe planar device, (b) A Ge-doped CdMgTe device, 1mm thick with 3mm dia. circular planar electrodes.

In general, Ge-doped detectors show much weak counting or no response at all in gamma spectral measurement. Even on sample that did show gamma response, the result was still typically not stable or exhibited significant degrading over time. Figure 29 shows the best Co-57 122 keV response that we can achieve so far on a 1mm planar Ge-doped sample. Again, as mentioned, this Ge-doped detector's response is also not stable. This characteristic of Ge-doped material is very different from that of In-doped ones'. For In-doped samples, when responded to gamma, the spectrum has been generally stable and repeatable. This might have a lot to do with the different role that the Ge atoms have in the compensation processes as compared to indium atoms' [22] Note that similar effect has been observed in CZT doping studies – Despite years of intense research by researchers in the wide band-gap semiconductor detector community, Ge-doped CZT has never demonstrated decent detector response, while In-doped CZT exhibited best detector response among all studied dopants. Due to limited time, we have not been able to measure the mu-tau for the responded post-anneal Ge-doped samples, but most of the non-responded ones' are likely below 10^{-4} cm^2/V and hence cannot be measured via the Am-241 TOF-gamma using the Hecht equation as we did with our In-doped sample shown in Figure 27. We managed, however, to get a measurement of a pre-anneal Ge-doped sample via TOF-laser where a value of 10^{-4} cm^2/V was obtained for electron. This is certainly a much smaller value than that of the good In-doped samples whose spectrum we presented in this report, where mu-tau for electron was very high, 5 x 10^{-3} cm^2/V as mentioned earlier.

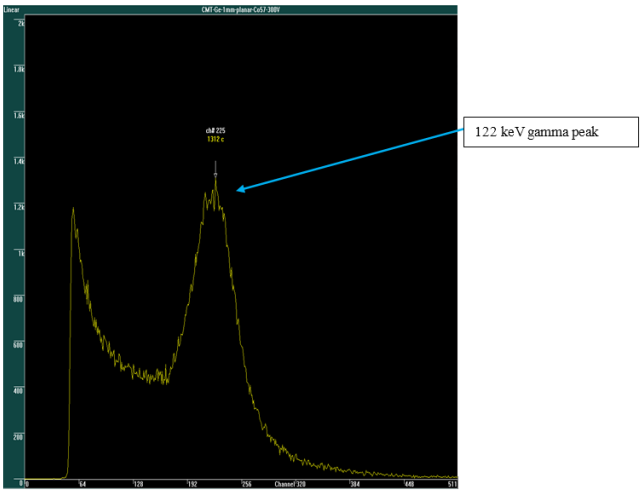

Figure 29. Best Co-57 response from a 1mm planar Ge-doped CdMgTe detector.

Thus, the fact that Ge-doped CdMgTe material has also been observed in our Phase 1 study so far, to be much worse compared to In-doped CdMgTe would not be too much of a surprise. This topic however, will likely be among the areas of further study in our Phase 2 plan.

Nevertheless, proper doping and growth conditions are not sufficient to produce gamma-ray detector material: **Proper post-growth annealing is also needed**. In fact, without this post-growth annealing process, materials having similar growth conditions have been observed to have much poorer gamma responses or even no response, as measured in the early stages of our phase 1 work. Post-growth annealing has also been used in other semiconductor detector materials such as CZT [23, 24]

The growth (including proper doping) and post-growth processing affect the electrical transport properties of the material, mainly resistivity and mobility-lifetime (or mu-tau), both mu-tau-electron and mu-tau-hole. It has been known that trapping and de-trapping associated with growth defects is a major factor limiting the performance of room temperature semiconductor detectors such as CdTe. By alloying CdTe with wide band-gap compound semiconductor with smaller lattice constant, one can harden it with respect to defect formation and hence produce a new compound with higher resistivity and mu-tau. And, of the three currently available candidates for alloying, Mg, Mn and Zn, Mg is a much better choice since CdTe-MgTe is more phase-diagram friendly (near similar lattice structure) compared to CdTe-ZnTe and CdTe-MnTe's and hence can lead to material with better crystallinity and better mu-tau potential. MgTe also has a bandgap close to 3.4 eV and hence CdMgTe can be tailored to have much wider bandgap than CdZnTe and CdMnTe (and hence higher resistivity). Furthermore, Mg's segregation coefficient in CdTe is nearly 1, so CdMgTe in theory can have better homogeneity. These favored factors certainly contribute a critical role in the detector performance. They are indication of good material quality especially electrical transport properties as confirmed by our mu-tau-electron measurement.

(2) The role of device design, fabrication and electronic instrumentation.

It is important to point out that the Cs-137 662 keV responses in Figure 20 to 23 as well as the Co-57 122 keV response in Figure 26 were all obtained with a Pseudo Frisch-Grid device configuration (See Figure 16a). This device configuration has also been known to be popular with CZT detectors. It is generally an electron-only type of device where electron collection efficiency is maximized and energy resolution is significantly enhanced due to the electric field focusing effect of the grid (copper-wrapping around the side walls) which steers all the charges drifted near the side walls back onto the collecting anode electrode. The performance of a planar device at this same thickness would not be as good unless the detector's thickness is much thinner as in Figure 24.

Thus, device design and configuration which generally involve aspect ratio of electrodes, size vs thickness, with or without single carrier focusing design play an important role in the usage of a material in radiation detection application. This fact is generally very well known in the radiation detection field and hence CdMgTe is no exception.

Another noteworthy point to mention is that surface preparations in device fabrication includes lapping/polishing, chemical etching, metallization as well as passivation has long been known to capable of causing detrimental effect in device performance [25,26]. Without proper fabrication procedures, a spectrometer-grade crystal will not exhibit good detector performance or even worse, exhibits very poor device responses. The detector whose responses shown via Figure 20 -27 in this report, all had proper fabrication and were well passivated. Had these steps been neglected, we would not have obtained the reported results. Though the fabrication processes have not been fully optimized during this Phase 1 work, this task will be one of the areas of research we propose during Phase 2 of this project.

Finally, electronic noise from the instrument system also contribute to the spectral broadening which is generally measured via the pulser width (FWHM in % just like energy resolution) as demonstrated in Figure 26. This electronics noise convolutes with the detector's intrinsic resolution, leading to the apparent detector energy resolution that one actually measures. If this electronic noise can be reduced, detector performance will certainly improve.

5.0 Conclusion and Future

In conclusion, this Phase I effort was aimed at exploring CdMgTe as a potential gamma-ray detector material. CdMgTe crystals were grown via the vertical Bridgman technique and samples were prepared for detector fabrication. Post-growth annealing was performed on the samples prior to detector fabrication, which was found to be a necessary requirement for successful detector operation. Modeling work was done during Phase I, the results of which will be further utilized in Phase II of this work to produce material with higher resistivity and improved transport properties.

The gamma-radiation detection response of CdMgTe was successfully demonstrated. Energy resolution in the 3% range has been achieved at 662 keV gamma from Cs-137 source, 6% at 122 keV from Co-57 source and 12% range at 59.6 keV along with lower energy x-ray peaks. All these results have been obtained at room temperature without any additional signal processing correction such as Depth of Interaction (DOI) Correction. Electron-mobility-lifetime value in our CdMgTe material is about 5.3 x 10-3 cm^2/V.

To the best of our knowledge, we are also the first to report "spectrometer-grade" gamma detector response from CdMgTe detectors over a wide range of gamma ray radiation, from below 60 keV to above 600 keV. These results are considered comparable to the existing technology of CdZnTe.

We have clearly demonstrated that CdMgTe material is an excellent choice for next generation room temperature gamma ray detection.

In Phase II we will expand upon this work and develop the procedures to manufacture and fabricate improved gamma-radiation detectors in a repeatable manner. Growth procedures, post-growth processing, dopant concentrations, etc., will be investigated in much greater detail.

With respect to the modelling work, the Phase I study relied on previously derived formation energies calculated with relatively small super cells. These calculations will be repeated with larger super cells, and will include the defects related to the presence of magnesium in the lattice, such as magnesium antisites and magnesium interstitials. Additionally, complexes of impurities with native defects have not been explicitly included in our initial study and, as discussed in the Results section, could account for discrepancies of our results with experimental findings. Finally, more work will be done to understand the role of re-equilibration that might occur as a crystal is cooled from its equilibration (growth or anneal) temperature to room temperature.

Along with further improving the quality of CdMgTe crystals for gamma ray detection, one of the aims of Phase II will be to develop a low cost production techniques for detector grade CdMgTe crystals. The cost driving factors for the current CZT material are poor yield (in case of high pressure Bridgman), extremely slow growth process (i.e. THM) and long time and efforts required in processing large volume crystals. We plan to focus our research to increase the yield of device quality crystal using Bridgman technique, which is more amenable in the case of CdMgTe. Moreover, we plan to optimize the growth and post processing conditions with the help of modeling work in order to improve the reproducibility.

Phase II, will also focus on process of device fabrication and manufacturing issues in much greater detail. The following processes will be investigated and optimized: lapping and polishing, chemical etching, metallization, passivation and encapsulation. The photolithography process for fabrication of pixelated devices will be investigated. Integration with electronics will be examined and long-term stability studies will be performed. Finally, scalable processes for large-scale fabrication and manufacturing of devices will be explored.

6.0 Bibliography/References Cited

[1] Alan Owens, A. Peacock. Nuclear Instruments and Methods in Physics Research A, 531 (2004) 18–37

[2] "Semiconductors for room temperature radiation detector applications," edited by R.B. James, T.E. Schlesinger, Paul Siffert and Larry Franks. *Materials Research Society Symposium Proceedings*, Volume 302, 1993.

[3] "Semiconductors for room temperature nuclear detector applications." Volume editors T.E. Schlesinger and R. B. James. *Semiconductors and Semimetals*, Volume 43. Treatise editors: R.K. Willardson, A.C. Beer and E.R. Weber, *Academic Press* (1995).

[4] L.A. Kosyachenko, A.V. Markov, E.L. Maslyanchuk, I.M. Rarenko, V.M. Sklyarchuk. Electronic and Optical Properties of Semiconductors, Vol. 37, No. 12 (2003) 1373.

[5] L.A. Kosyachenko, O.L. Maslyanchuk, I.M. Rarenko, V.M. Sklyarchuk, *Phys. Stat. Sol. (c)* 1, No. 4 (2004) 925.

[6] V.M. Zalentin, Atomic Energy, Vol. 97, No. 5 (2004) 773.

[7] A. Owens, *Journal of Synchrotron Radiation 13*, (2006) 143.

[8] J. Steininger, A. J. Strauss and R.F. Brebrick. *J. Electrochem. Society*, Vol. 117, No. 10, P. 1305 (1970).

[9] A. Mycielski, A. Burger, M. Sowinska, M. Groza, A. Szadkowski, P. Wojnar, B. Witkowska, W. Kaliszek, O. Siffert, *Phys. Stat. Sol. (c)* 2 (2005) 1578.

[10] A. Burger, K. Chapttotadhyay, H. Chen, J.-O. Ndap, X. Ma, S. Trivedi, S.W. Kutcher, R. Chin, and R.D. Rosemeier, *Journal of Crystal Growth* 198/199 (1999) pg 72.

[11] Giuseppe Camarda, "Characterization of Detector Grade CdTeSe Crystals", Presented at the 2013 MRS Spring Meeting & Exhibit, April 1-5,2013April 2013

[12] Sudhir B. Trivedi, Chen-Chia Wang, Susan Kutcher, Uwe Hommerich, and Witold Palosz, "Crystal Growth Technology of Binary and Ternary II-VI semiconductors for Photonic Applications,J.Cryst.Growth 310(2008)1099-1106

[13] A.Hossain, V. Yakimovich, A. E. Bolotnikov, K. Bolton, G. S. Camarda, Y. Cui, J. Franc, R. Gul, K-H Kim, H. Pittman, G. Yang, R. Herpst, and R. B. James, "Development of Cd(1-x)MgxTe for Room Temperature X- and Gamma Ray Detectors, J.Cryst.Growth,379(2013)34-40

[14] K. Itoh, "Preparation and some properties of solid solutions $Cd_{1-x}Mg_xTe$". J. Phys. Soc. Japan 22 (1967) 1,119.)

[15] Leonel P. Gonzalez, Shekhar Guha, Mark Corbett, Sudhir Trivedi. "Comparison of the nonlinear transmission of $Cd_{0.65}Mg_{0.35}Te$ and CdTe". Quantum Electronics and Laser Science Conference, 2005. QELS '05, Vol 2.

[16] Y.S. Ihn, T.J. Kim, Y.D. Kim, D.E. Aspnes, J. Kossut. "Optical properties of $Cd_{1-x}Mg_xTe$ (x=0.00, 0.23, 0.31, and 0.43 alloy films" Applied Physics Letter, Vol. 84, Issue 5, pp. 693-695 (2004).

[17] Eunsoon Oh, C. Parks, I. Miotkowski, M. Dean Sciacca, A.J. Mayur and A.K. Ramdas."Optical properties of Mg-based II-VI ternaries and quaternaries: $Cd_{1-x}Mg_xTe$ and $Cd_{1-x-y}Mg_xMn_yTe$. Physical Review B, Volume 48, Number 20, pp 41-45 (1993).

[18] "Development of CdMgTe and CdMgSe for optical switching applications" Contract #FA8650-11-C-5116, Monitored by Wright Patterson Air Force Base, Program Manager-Arlynn Hall, Technical Monitor- Leonel Gonzalez (Jan 2011- Jan 2013).

[19] Kroger, F. A. “The Chemistry of Imperfect Crystals”, John Wiley & Sons, Inc., New York (1964).
[20] Berding, M. A., M. van Schilfgaarde, and A. Sher, “First-principles calculations of native defects in HgCdTe”, Physical Review B 50, 1519 (1994).
[21] Berding, M. A., “Annealing conditions for intrinsic CdTe.” Applied Physics Letters 74, 552 (1999).
[22] Fiederle, M. et. al. “Comparison of undoped and doped high resistivity CdTe and (Cd, Zn) Te detector crystals”, IEEE Trans. Nucl. Sci. Vol 51, No. 4, pp. 1864-1868, August, (2004).
[23] Yu, P. F., Jie, W. Q., “Effects of H2 Atmosphere Annealing on the properties of CZT:In Single Crystals”, J. Elec. Mat. Vol 42, No 12, pp. 3385-3389, (2013).
[24] Yu, P., Jie, W., “Effects of post-growth annealing on the performance of CdZnTe:In radiation detectors with different thickness”, Nucl. Instr. Meth. A, 737, pp. 29-32 (2014).
[25] Chen, H. et. al., “Passivation of CdZnTe Surface by Oxidation in Low Energy Atomic Oxygen”, J. Vac. Sci. techno. A 17(1), pp. 97-101, Jan/Feb (1999).
[26] Burger, A., et. al., “Investigation of Electrical Contacts for CdZnTe Nuclear Radiation Detectors”, IEEE Trans. Nucl. Sci. Vol 44, No. 3, pp. 934-938, June (1997).